Annu. Rev. Pharmacol. Toxicol. 2021. 61:X–X
https://doi.org/10.1146/annurev-pharmtox-061220-093932

*These authors contributed equally to this article
Sivaraman et al.

Structural Basis of the SARS-CoV-2/SARS-CoV Receptor Binding and Small-Molecule Blockers as Potential Therapeutics

Hariharan Sivaraman,* Shi Yin Er,* Yeu Khai Choong, Edem Gavor, and J. Sivaraman

Department of Biological Sciences, National University of Singapore, Singapore 117543; email: dbsjayar@nus.edu.sg

Abstract

Over the past two decades, deadly coronaviruses have caused major challenges to public health, with the most recent being the severe acute respiratory syndrome-related coronavirus-2 (SARS-CoV-2, 2019) pandemic. The path for virus invasion into humans and other hosts is mediated by "host-pathogen" interactions, specifically, virus-receptor binding. An in-depth understanding of the virus-receptor binding mechanism is a prerequisite for the discovery of vaccines, antibodies, and/or small-molecule inhibitors that can interrupt this interaction and prevent or cure infection. In this review, we discuss the viral entry mechanism, the known structural aspects of virus-receptor interactions (SARS-CoV-2 S/humanACE2, SARS-CoV S/humanACE2, and MERS-CoV S/humanDPP4), the key protein domains and amino acid residues involved in binding, and the small-molecule inhibitors and other drugs that have (as of June, 2020) exhibited therapeutic potential. Specifically, we review the potential clinical utility of two transmembrane serine protease 2 (TMPRSS2)-targeting protease inhibitors, nafamostat mesylate and camostat mesylate, as well as two novel potent fusion inhibitors and the repurposed Ebola drug, remdesivir, which is specific to RdRp, against human coronaviruses, including SARS-CoV-2.

1. CORONAVIRUS OUTBREAKS

The propensity of coronaviruses to exhibit interspecies and cross-species transmission is chiefly determined by the virus' ability to bind to the receptors of new hosts (1–4). This transmissibility has resulted in the outbreak of many zoonotic coronaviruses, such as SARS-CoV in 2003, MERS-CoV in 2012, and the current SARS-CoV-2 pandemic, which emerged in 2019 (5, 6). These three *betacoronaviruses* have caused major respiratory diseases in humans, with clinical symptoms ranging from the common cold and fever to severe lung injuries and even death. Given that there are currently no antivirals or vaccines against any of these three viruses (7), there remains an urgent need for the design and testing of effective treatment and preventive options.

Since the emergence of SARS-CoV-2—the pathogen responsible for coronavirus disease (COVID-19)—many therapeutic regimens are being explored with the help of data garnered previously during SARS-CoV and MERS-CoV epidemics. While vaccines remain the ultimate strategy for infection prevention, the timeline for their production may not be favourable for the COVID-19 pandemic. Alternative therapeutics such as neutralizing antibodies and small-molecule inhibitors are therefore urgently needed, and many of these have been approved for clinical trials. Drugs like remdesivir (Gilead Sciences), a repurposed drug for Ebola, and ritonavir and lopinavir, two repurposed drugs used for HIV, have been approved by regulatory authorities for early-phase clinical trials (8). Other early interventions, such as convalescent plasma from patients who have recovered from COVID-19 and antisera from immunized rodents, have been explored with conflicting results (2, 9, 10).

1.1. Spike S-glycoprotein

Coronaviruses are positive-sense, single-stranded RNA viruses (11). Their 26–32 kb genomes encode for a polyprotein chain made up of 16 nonstructural proteins and 4 structural proteins, of which the spike (S)-glycoprotein is the key surface protein that facilities host cellular interaction and entry (12). The S-glycoprotein comprises two proteolytically activated subunits: S1 subunit, comprising the N-terminal domain (NTD) and a receptor-binding domain (RBD), also known as the C-terminal domain (CTD), and an S2 subunit. (13). The RBD engages the host receptor whereas the S2 subunit is responsible for membrane fusion (14). Crystal and cryo-electron microscopy (cryo-EM) structures of the S-glycoprotein reveal its homotrimeric conformation

with the S1 and S2 subunits present in each monomeric unit (2, 15).

1.2. Human Receptors

Exceptionally, coronaviruses from the same genus utilize different receptors and coronaviruses from different genera can utilize the same receptor (1, 16, 17). SARS-CoV, MERS-CoV, and the current SARS-CoV-2 all belong to the same genus of *betacoronaviruses.* SARS-CoV and SARS-CoV-2 recognize angiotensin converting enzyme 2 (ACE2) whereas MERS-CoV recognizes dipeptidyl peptidase 4 (DPP4) (2, 3, 16). These factors, if extensively explored, could shed light on coronavirus pathogenesis, its cross-species potential, the infection process, and ultimately lead to ways to effectively predict zoonotic outbreaks and block future virus-receptor interactions.

1.3. Pathogen-receptor Recognition and Small-molecule Inhibitors

Many structures of the RBD-ACE2 (Protein Data Bank IDs (PDB IDs): 3D0G, 6VW1) (11, 18–20) and RBD-DPP4 (PDB ID: 4L72) (16) complexes exist, thus providing a structural basis for the development of therapeutic agents (**Table 1**). Furthermore, the biochemical characterization and complex structures of small-molecule inhibitors (PDB IDs: 6LZE, 7BQY, 7BUY, 6Y2F, 7BV2) (21–24) that target various pathways of the virus—entry, replication, and assembly—have been determined and can be used to elucidate how these molecules act as therapeutic agents against SARS-CoV-2 (**Table 2**). Drawing cues from available virus S-glycoprotein-human receptor interactions, this review seeks to provide a mechanistic basis for receptor usage by SARS-CoV, MERS-CoV and SARS-CoV-2. Drawing on knowledge from SARS-CoV- and MERS-CoV-associated therapies, we also analyze the molecular basis of blocking SARS-CoV-2 by various therapeutic small-molecule drugs. Thus, this article provides a foundation for the development of new therapeutic and preventive strategies, and proposes potential ways to improve existing strategies, such as vaccines and antibodies, and the use of small-molecule drugs, against COVID-19.

2. SARS-COV-2, SARS-COV, AND MERS-COV ENTRY MECHANISM

Viruses enter hosts by fusion or endocytosis. During fusion, the virus attaches to and connects with the cell membrane, a process mediated by the binding of viral proteins (S -glycoprotein) to host cell receptors (human ACE2 or DPP4). This leads to the formation of an immune-resistant

protein complex that can cross membrane barriers. In contrast, in receptor-mediated endocytosis, the viral particle attaches to the cell membrane using S-glycoproteins as attachment factors and is engulfed by the cell membrane as vesicles, a process mediated by the host-cell receptors (25). Recent work demonstrates that SARS-CoV-2 enters host cells via endocytosis (26). Qian and colleagues suggest that phosphatidylinositol 3-phosphate 5-kinase (PIKfyve), a two-pore channel subtype 2 (TPC2), and cathepsin L are crucial for SARS-CoV-2 entry (26). By comparison, SARS-CoV enters host cells via a clathrin- and caveolae-independent, receptor- and pH-dependent mechanism of endocytosis (27). Using confocal microscopy, Jiang and colleagues showed that hACE2 translocates from the cell surface into intracellular compartments after treatment with pseudovirus harboring the S-glycoprotein in SARS-CoV (27). The transmembrane serine protease 2 (TMPRSS2) is thought to cleave the SARS-CoV S-glycoprotein after it undergoes a conformational change upon binding to hACE2, exposing the cleavage site near the C-terminus (28, 29). MERS-CoV entry into the host is dependent on cysteine protease cathepsin-L in the presence of uncleaved pseudovirions (30, 31). Using guided protease expression and inhibition assays, Pohlmann and colleagues showed that TMPRSS2 activates the S-glycoprotein in human coronavirus EMC (hCoV-EMC) and mediates cathepsin B/L-independent host cell intrusion, similar to the mode of entry described for SARS-CoV (31–33).

3. SEQUENCE FEATURES AND HIGHER TRANSMISSIBILITY EXHIBITED BY SARS-COV-2

SARS-CoV-2 harbours an arginine-rich multibasic cleavage site (also known as the RRAR furin cleavage site) that is sensitive to furin, an enzyme present in host cells (3, 12, 34). This site is not found on SARS-CoV. Through mutational analysis, Pohlmann and colleagues confirmed that the furin cleavage site must remain intact for high-efficiency proteolytic processing of the SARS-CoV-2 S-glycoprotein and efficient entry into host cells (35). The addition of an Arg residue along with an Ala to Lys replacement in the SARS-CoV-2 S-glycoprotein showed no enhanced cleavability (35). Thus, the multibasic furin cleavage site in SARS-CoV-2 S-glycoprotein appears to be necessary for high-fidelity proteolytic processing.

During viral infection, syncytia formation is a phenomenon that occurs when infected cells fuse with neighboring cells to result in large, multinucleated cells. To establish the critical role of

the multibasic furin cleavage site in syncytia formation, Pohlmann and colleagues performed mutational experiments and syncytia formation assays (35). SARS-CoV-2 S-glycoprotein and MERS-CoV S-glycoprotein showed syncytia formation, which increased in the presence of trypsin and expression of TMPRSS2. In the absence of the multi-basic furin cleavage site, syncytia formation was remarkably reduced, even in the presence of trypsin or TMPRSS2. Whereas SARS-CoV wild type (WT) expression did not establish syncytia formation, SARS-CoV WT in the presence of furin cleavage sites showed syncytia formation and enhanced cell-cell fusion (36). Overall, these findings reveal the importance of the furin cleavage site in cell-cell fusion and high-fidelity proteolytic processing and suggest the utility of inhibitors targeting furin or TMPRSS2 as potential therapeutic options.

The K_d of SARS-CoV-2 RBD/hACE2 interaction is in the lower nM range (**Table 1**) (18, 19). This strong affinity could be another reason why SARS-CoV-2 spreads faster.

Moreover, SARS-CoV-2 infects people of different age groups and demographics, but differences in infectivity and severity are reported between men versus women and adults versus children (37). This disparity may be attributed to the difference in hACE2 expression among different age groups and gender. In men, hACE2 expression is believed to be higher due to it being located in the X-chromosomes (37). Comparing adults versus children, enhanced hACE2 expression was observed in well-differentiated cells (adults) compared to poorly differentiated cells (children) (37, 38). Though suggestive, these claims need substantiation with further experimental evidences.

4. STRUCTURAL INSIGHTS ON VIRUS-RECEPTOR INTERACTIONS

Biochemical characterization and structural analysis have provided insights into the molecular conformations of hACE2 and hDPP4 and provided clues as to how they interact with the S-glycoprotein. hACE2 comprises an active N-terminal peptidase domain with two lobes, resembling a claw-like structure, and a C-terminal collectrin domain that can assume both "opened" and "closed" conformations (39). The SARS-CoV RBD can bind to hACE2 irrespective of the conformation assumed by hACE2 (20). Four key residues in hACE2 govern the interaction—Lys31, Glu35, Asp38, and Lys353—of which Glu35 is conserved across numerous species (e.g., in domestic cats, ferrets, monkeys, and raccoons) (11).

The human host-cell receptor hDPP4 consists of an N-terminal 8-bladed β-propeller domain

(39–496), with each blade formed by 4 antiparallel β-strands and a C-terminal hydrolase domain (497–766) (16). The hDPP4 blades interact with MERS-CoV. Akin to SARS-CoV, the MERS-CoV S-glycoprotein comprises an NTD and an RBD consisting of 84 residues folded into 4-stranded antiparallel β sheets (aa 484 to 567) (16). Several key residues in the hDPP4 β-propeller domain (Val26, Arg336 and Arg317) interact with the MERS-CoV RBD residues (Asp510, Glu536, Asp537 and Asp539) through a network of hydrophilic and hydrophobic interactions (16).

SARS-CoV-2 and MERS-CoV have a furin cleavage site and are cleaved for attachment and pathogenesis. During fusion with the host, the S1 and S2 subunits of the MERS-CoV S-glycoprotein separate. The S2 subunit forms a six-helix fusion bundle [6-HB: heptad repeat (HR)-1 (a.a 987–1062) and HR2 (a.a 1263–1279) region] that fuses with the host-cell membrane (40). SARS-CoV and MERS-CoV have high sequence identity in the NTD, but poor conservation of the RBD, which may explain their different host-cell receptor specificity (16).

As does the S-glycoprotein of SARS-CoV, the S-glycoprotein of SARS-CoV-2 engages with hACE2 under neutral pH conditions for fusion and entry into host cells (18–20, 41). The SARS-CoV-2 S-glycoprotein has 22 N-linked glycosylation sites that are spread throughout the different domains, including the NTD (at positions 1, 4, 122, 149, 165, 234, 282) and RBD (at positions 331 and 343) (42). An analysis of the X-ray and cryo-EM structures published by different groups points to the RBD as the key region that interacts with hACE2 (**Table 1**) in a 1:1 ratio (one SARS-CoV-2 RBD molecule binding to one hACE2 receptor molecule); the SARS-CoV-2 NTD, in the absence of RBD, is unable to bind to hACE2 (2).

The SARS-CoV-2 RBD consists of five antiparallel β sheets (β1, β2, β3, β4, and β7), and two short β strands (β5 and β6) situated between β4 and β7, connected by short helices (α4 and α5) and loops (18). Most of the hACE2-interacting residues lie in the region formed by α4 and α5 helices, β5 and β6 sheets, and the connecting loops, collectively labeled as the receptor binding motif (RBM) (2, 18, 19). More than 16 residues in the RBD interact with hACE2: 8 residues are unique to SARS-CoV and 9 to SARS-CoV-2 (**Figure 1*c***) (18). Conversely, 20 key residues in hACE2 interact with the RBD, with only 1 and 2 unique to SARS-CoV-2 and SARS-CoV, respectively (**Figure 1d**) (2). Superimposition of the RBD structures of SARS-CoV and SARS-Cov-2 shows a root-mean-square deviation value of 0.475 Å for 128 equivalent Cα atoms (2).

In addition to the hydrogen bonding contacts, there is a network of hydrophobic interactions formed by residues Phe486 and Tyr489 in SARS-CoV-2 RBD and Phe28, Leu79, Met82, and Tyr83 residues in hACE2 (2). A key receptor-interacting residue, Lys417, situated outside the SARS-CoV-2 RBM, forms a salt-bridge with Asp30 of hACE2. For SARS-CoV RBD, Lys417 is replaced by a valine residue, which does not interact with hACE2 (18).

In the SARS-CoV-2 RBM, an hACE2-interacting loop (a 4-residue motif, GVEG) adopts a favourable conformation for binding, which differs from that of the SARS-CoV RBM (3- residue motif, PPA) (2, 19). Mutations introduced into the hACE2 binding loop of the SARS-CoV-2 RBM showed reduce its affinity, confirming the critical role of the loop in receptor binding (19).

The nM range of the binding affinity between hACE2 and the SARS-CoV-2 RBD—as determined by surface plasmon resonance (SPR) and bio-layer interferometry (BLI) experiments—point to the critical role of the RBD in host cell receptor binding (2). Even though discrepancies have been reported by different groups regarding the affinity of this binding, presumably due to differences in experimental protocols, all the K_d values are in the nM range. Wang and colleagues reported that the SARS-CoV-2 RBD has a fourfold stronger affinity for hACE2 than does the SARS-CoV RBD (2). This could be due to the different conformational states adopted by the SARS-CoV S-glycoprotein: its receptor-binding inactive state and active state. In the inactive state, the RBDs are pointed downward, which causes a steric clash that inhibits its interaction with hACE2. In contrast, in the active conformation, the RBDs point upward, presenting the binding site and thus facilitating hACE2 binding (43, 44).

Although the mode of binding exhibited by the RBD with hACE2 is comparable between the two viruses (18), the RBM of the SARS-CoV-2 S-glycoprotein forms a broader binding interface, establishing more contacts with hACE2 (2, 19). This might explain the higher binding affinity of the SARS-CoV-2 RBD and hACE2.

The presence of many hydrophilic interactions, governed by salt-bridges and hydrogen bonds, are a common feature between the SARS-CoV-2 RBD/hACE2 and SARS-CoV RBD/hACE2 interfaces (2, 18).

Experiments have been performed to determine if the antibodies raised against the SARS-CoV S1 subunit could neutralize SARS-CoV-2. Most results have been disappointing, with little to no cross-neutralization for many of the antibodies, indicating that there is likely to be crucial differences in antigenicity (2), but some SARS-CoV-2- and SARS-CoV-derived antibodies (45–

47) have shown promising neutralizing activities against SARS-CoV-2. Because the SARS-CoV and SARS-CoV-2 S-glycoproteins bind to ACE2 and not hDPP4, which is specific for MERS-CoV (2), it is unlikely that any of the MERS-CoV antibodies will offer any promise.

Analyses of the published mutational studies, flow cytometry, colocalization, biochemical data and structures have suggested that the SARS-CoV-2 S-glycoprotein shows a more favourable interaction with hACE2 than does the SARS-CoV S-glycoprotein. Although the structures of the S-glycoprotein–receptor complexes are similar, it remains unclear whether structural differences are the sole reason for the faster transmissibility of SARS-CoV-2 between hosts. Another important finding to consider is the difference in the antigenicity and immunogenicity between SARS-CoV-2 and SARS-CoV S-glycoproteins.

5. CURRENT STATUS OF POTENTIAL SMALL-MOLECULE COMPOUNDS AVAILABLE AGAINST SARS-COV-2

There is no effective drug or vaccine currently available for COVID-19. Clinically approved drugs with published safety profiles represents the fastest option to discover an effective therapy, particularly during a pandemic. Clinically approved drugs are being repurposed as potential treatment options for COVID-19 (48, 49).

Several recent reports that include new compounds and repurposed drugs appear to have great potential against SARS-CoV-2 infection. Some of these candidates were also tested against SARS-CoV and MERS-CoV. These antivirals exert their activity by inhibiting viral entry and fusion pathways, blocking viral proteases important for viral transcription, and targeting host factors that are essential for viral replication (**Figures 2** and **3**). Here and in the tables, we discuss the current status of potential drugs available for this ongoing pandemic of SARS-CoV-2 (**Tables 2** and **3**).

5.1. Targeting Viral Entry via the Endosomal Pathway

Following hACE receptor binding and endocytosis, acidification of the internalized endosome is required to retrieve the internalized cargo proteins and viral RNAs that support coronavirus replication (50–53). Lysosomal cathepsins are essential for SARS-CoV-2, SARS-CoV, and MERS-CoV entry via endocytosis (26). Fusion activation by cathepsin L cleavage of the SARS-CoV-2 S-glycoprotein is similar to that observed for SARS-CoV and MERS-CoV (26, 30, 54).

The literature has discrepancies regarding the role of autophagy in coronavirus infection (55).

Studies have shown that SARS-CoV and MERS-CoV block the fusion of autophagosomes and lysosomes, and suppress the autophagy process (56, 57). Induction of autophagy has an antiviral effect on SARS-CoV-2 and MERS-CoV replication (57–59) but exactly how autophagy suppresses viral replication remains to be determined (60).

5.1.1. Drugs Targeting Endosome Acidification.

Lysosomotropic agents, such as hydroxychloroquine, chloroquine and ammonium chloride, inhibit SARS-CoV-2 and SARS-CoV replication by increasing lysosome pH and thus interfering with virus-cell fusion (61–64). During the early COVID-19 outbreak, the malaria drugs, chloroquine and hydroxychloroquine, were among the first few inhibitors to be taken to clinical trials (65–67). However, emerging information have questioned the benefit of these drugs.

Omeprazole is another lysosomotropic agent that has been tested for its efficacy against SARS-CoV-2. Omeprazole is a proton pump inhibitor that interferes with lysosomal activity through inhibition of H^+, K^+-ATPase and resultant alkalization of the phagolysosome, which, in turn, inhibits virion fusion and thus viral replication (**Figure 2*a,i***) (68–70). In addition, omeprazole also inhibits double-stranded RNA formation, thereby preventing viral replication (8). Omeprazole inhibits SARS-CoV-2- and SARS-CoV-induced cytopathogenic effect formation (CPE) at an IC_{50} of 27–34 μM (8). However, those concentrations are beyond acceptable therapeutic plasma concentration (71). Combining omeprazole with other inhibitors may produce the desired therapeutic response. A combination of aprotinin and omeprazole at the therapeutic concentration enhances aprotinin-mediated SARS-CoV-2-induced CPE formation by 2.7 fold (IC_{50} = 10.4 μM). Simultaneous administration of omeprazole with remdesivir, at therapeutic concentrations, increases remdesivir-mediated inhibition activity by tenfold (IC_{50} = 0.023 μM) (8).

5.1.2. Drugs Targeting Cathepsin.

E64d, a broad-spectrum cysteine protease inhibitor, targets lysosomal cathepsin. E64d has been widely used in studies of endosome-mediated viral entry (**Figure 2*a,i***). For example, E64d reportedly reduces the entry of SARS-CoV-2 pseudovirus into HeLa/hACE2, Calu-3, and MRC-5 cells (72), of SARS-CoV-2 S- pseudovirus entry into 293/hACE2 by 92% (26) and of pseudotyped SARS-CoV S-glycoprotein (73). Hoffmann et al. reported that the TMPRSS2 inhibitor camostat mesylate partially blocks SARS-CoV-2 S-glycoprotein-mediated entry into

target cells, and that combined treatment with E64d could fully block viral entry (34). As SARS-CoV-2 can utilize both cathepsin L and TMPRSS2 for S-glycoprotein priming (26, 34, 74), E64d has the potential to be developed as an anti-SARS-CoV-2 drug and used in combination with a TMPRSS2 inhibitor to achieve a cumulative antiviral effect.

5.1.3. Drugs Targeting the Autophagy Pathway.

Spermidine is a natural polyamine that induces autophagy (**Figure 2*a,ii***) (75–78). Its concentration declines in response to SARS-CoV-2-induced inhibition of spermidine synthase (58). Gassen et al. reported that the supplementation of spermidine can enhance autophagy and suppress SARS-CoV-2 propagation by 85% in vitro (58). Polyamines also play pivotal roles in viral genome synthesis, including transcription, translation and genome packaging (60). Studies in chikungunya virus (CHIKV), Zika virus (ZIKV), hepatitis C virus (HCV) and Ebola virus highlight the enhancement of viral polymerase activity by polyamines (79–82). Further investigation is needed to understand the role(s) of spermidine in SARS-CoV-2 infection.

AKT1, which can be inhibited by MK-2206, targets Beclin 1, an autophagy induction protein (83, 84). Inhibition of AKT1 with MK-2206 leads to an up-regulation of Beclin 1 and promotes autophagy. Thus, MK-2206 may be a promising drug candidate for the treatment of SARS-CoV-2 infection. MK-2206 reduced SARS-CoV-2 propagation by 88% (58).

Gassen et al. reported that MERS-CoV replication could be reduced by inhibiting S-phase kinase-associated protein 2 (SKP2), an E3-ligase that suppresses autophagy via Beclin 1-mediated ubiquitination. (57). A recent preprint from the same group of researchers identified niclosamide—an orally bioavailable, chlorinated salicylanilide used to treat tapeworm—as a potential anti-SARS-CoV-2 agent (58). Niclosamide inhibits SKP2, stabilizes Beclin-1 and enhances autophagy (57, 58). Niclosamide also is a protonophore that blocks endosomal acidification, which is essential for virion fusion (85). Another group also reported antiviral activity of niclosamide against SARS-CoV-2 (IC_{50} = 280 nM) (86). As an FDA-approved anthelminthic drug used in humans for more than 40 years (87, 88), niclosamide has a known safety profile and can be tested in animal models and clinical trials against SARS-CoV-2.

5.2. Targeting Viral Entry Through Plasma Membrane Fusion Pathway

The plasma membrane fusion pathway is an essential part of viral infection, and thus a potential candidate target for virus pathogenicity. Unlike most betacoronaviruses, the S-glycoprotein of

SARS-CoV-2 has a multibasic S1/S2 proprotein convertase furin-cleavage site (35). In the plasma membrane fusion pathway, SARS-CoV-2 uses furin and the TMPRSS2 serine protease for S-glycoprotein priming: furin cleaves S-glycoprotein at the S1/S2 site whereas TMPRSS2 targets the S2 site (35, 89). Hence, TMPRSS2 is a target for serine protease inhibitors to block S-glycoprotein cleavage and block viral entry. Furin and TMPRSS2 are both essential and cannot compensate for each other in S-glycoprotein activation (89). Therefore, drugs targeting either (or perhaps both) of these proteases involved in the plasma membrane fusion pathway may suppress S-glycoprotein activation and viral entry.

During viral pathogenesis, membrane fusion is instigated by the formation of a 6-helical bundle (6-HB) fusion core. Upon hACE2 receptor binding, the HR1 and HR2 domains in the S2 subunit of the S-glycoprotein interact with each other to form the core (90–92); the viral and cell membranes are driven into close proximity by its formation. Thus, inhibitors that target 6-HB fusion core formation may also prove useful against membrane fusion to prevent viral entry (**Figures 2*a*,*v*** and **3*a***).

5.2.1. Drugs targeting furin and TMPRSS2 proteases.

Bestle et al. showed that the synthetic furin inhibitor, MI-1851 potently inhibits S-glycoprotein cleavage and SARS-CoV-2 replication (**Figure 2*a*,*iii***) (89). In human Calu-3 airway cells infected with SARS-CoV-2, MI-1851 reduced viral titers by 30- to 75-fold, and this effect could be enhanced when delivered in combination with various TMPRSS2 inhibitors (89).

Numerous repurposed TMPRSS2 inhibitors have been shown to block SARS-CoV-2 S-glycoprotein mediated entry (**Figure 2*a*,*iv***). Two such inhibitors are camostat mesylate (34), which is approved for the treatment of pancreatitis (93) and postoperative reflux esophagitis in Japan, and nafamostat mesylate, which is approved by the FDA for treating pancreatitis (94). Compared with camostat mesylate, nafamostat mesylate has a >15-fold lower concentration-response (**Table 2**) for inhibition of SARS-CoV-2 entry (95). Nafamostat mesylate has also been identified as a potent inhibitor of MERS-CoV infection (96). Currently, both of these compounds are being evaluated in clinical investigations for the treatment of SARS-CoV-2.

Aprotinin in aerosol form, which delivers drugs directly to the lungs, is approved for influenza treatment in Russia (97). Bojkova et al. reported that, at therapeutic concentrations, aprotinin shows higher inhibition of SARS-CoV-2 than SARS-CoV infection. (8). This might be due to the differentially conserved amino acid positions (DCPs) between the S-glycoprotein of

SARS-CoV-2 and SARS-CoV (8). In addition, aprotinin shows a higher antiviral effect than camostat and nafamostat and in contrast to those compounds, aprotinin also interferes with formation of double-stranded RNA, thereby preventing viral infection in SAR-CoV-2-infected cells (8). Aprotinin may thus be a promising drug candidate, based on its efficacy at therapeutic concentration and its safety in terms of its mode of administration.

Another serine protease inhibitor, MI-432, is a synthetic peptide mimetic inhibitor of TMPRSS2 (98). MI-432 suppresses SARS-CoV-2 multiplication and CPE in Calu-3 human airway cells. In addition, the combination of MI-432 and the furin inhibitor, MI-1851, has an increased anti-SARS-CoV-2 activity as compared to treatment with single inhibitor (8).

5.2.2. Drugs targeting HR1 of S2 subunit of S-glycoprotein.

On the basis of the X-ray crystal structure of the 6-HB fusion core of the SARS-CoV-2 S-glycoprotein (PDB: 6LXT) and a pan-coronavirus fusion inhibitor EK1 peptide (99), Xia et al. developed a potent fusion inhibitor, EK1C4 lipopeptide, which targets SARS-CoV-2 S-glycoprotein-mediated cell membrane fusion, as well as pseudotyped SARS-CoV-2 and live SARS-CoV-2 infection with IC_{50} values of 1.3 nM, 15.8 nM, and 36.5 nM, respectively (100). Both EK1 and EK1C4 disrupt 6-HB fusion core formation by binding to the HR1 domain and show broad-spectrum fusion-inhibitory activity against SARS-CoV-2, SARS-CoV, and MERS-CoV, as well as against human coronavirus (HCoV)-OC43, HCoV-NL63, and HCoV-229E (**Figures 2*a*,*v*** and **3*a***) (100, 101). By modifying EK1 with a cholesterol moiety, EK1C4 forms a more stable complex with HR1, which enhances its antiviral activity (149-fold). Furthermore, the high selectivity index of EK1C4 (SI > 136) suggests that it is a potential inhibitor with little to no toxic effect in vitro. IPB02, another lipopeptide fusion inhibitor that targets the HR1 region, was designed based on the HR2 sequence (102). This inhibitor also potently inhibits the cell fusion activity of SARS-CoV-2 S-glycoprotein (IC_{50} = 25 nM) and SARS-CoV-2 pseudovirus (IC_{50} = 80 nM). In both cases, conjugating the peptides with cholesterol enhanced the antiviral effects and HR1 binding stability (100, 102). This cholesterol modification strategy has also been used in HIV inhibitors (103, 104).

5.3. Targeting the Main Protease

The main protease, M^{pro}, also known as 3C-like protease ($3CL^{pro}$), is a 33.8-kDa cysteine protease that mediates viral replication and transcription (105). M^{pro} is highly conserved among

all the coronaviruses, especially the substrate-binding site and the active site Cys145-His41 catalytic dyad (22, 106–110). The two polyproteins pp1a and pp1ab are cleaved by papain-like protease (PL^{pro}) and M^{pro} into 16 nonstructural proteins (NSPs) which are essential for envelope (E), membrane (M), spike (S), and nucleocapsid (N) protein production (111, 112). Absence of a human homolog and the availability of the apo structure (PDB ID: 6Y2E) as a template, make M^{pro} an attractive target for antiviral drug design (**Figures 2*b,i*** and **3*b***) (23, 107, 108, 113, 114).

Recently, Dai et al. designed and developed two structure-based anti-SARS-CoV-2 compounds that target M^{pro}: 11a and 11b. The X-ray crystal structures of SARS-CoV-2 M^{pro} in complex with 11a (PDB ID: 6LZE) and 11b (PDB ID: 6M0K) were determined at 1.5-Å resolution. Although differences in the chemical structure were observed—a cyclohexyl group for 11a versus a 3-fluorophenyl group for 11b—the compounds demonstrated a similar inhibitory mechanism: they occupy the substrate-binding pocket and the aldehyde group of the compounds covalently binds to the catalytic site Cys145, and blocks enzymatic activity of M^{pro} (21). 11a and 11b display high SARS-CoV-2 M^{pro} inhibitory activity (IC_{50} values = 53 nM and 40 nM, respectively (21)). The high selectivity indices for 11a (SI > 189) and 11b (SI > 139) indicate that these compounds offer good antiviral activity without significant cytotoxic effects.

N3, a Michael acceptor inhibitor, was previously shown to strongly inhibit SARS-CoV, MERS-CoV and infectious bronchitis virus in animal models (107). Jin et al. recently solved the crystal structure of N3 in complex with SARS-CoV-2 M^{pro} at 2.16-Å and 1.7-Å resolution (PDB ID: 6LU7; 7BQY) (22). N3 binds irreversibly in the M^{pro} substrate-recognition pocket and inhibits SARS-CoV-2 with an EC_{50} value of 16 μM.

Two other drugs have been shown to act by affecting M^{pro}: Ebselen and carmofur. These drugs were identified as potential drugs against SARS-CoV-2 through high-throughput screening (22). Ebselen has been studied in clinical trials for noise-induced hearing loss and bipolar disease (115–117), whereas carmofur is approved for adjuvant chemotherapy of colorectal cancer in some countries, and used clinically to treat breast, gastric and bladder cancer (118–121). Tandem MS/MS analysis revealed that ebselen and carmofur covalently bind to the catalytic Cys145 of SARS-CoV-2 M^{pro}. Carmofur completely modifies M^{pro} whereas ebselen only partially modifies it. Intriguingly, ebselen shows better inhibition than carmofur (IC_{50} = 0.67 μM versus 1.82 μM), suggesting it may inhibit M^{pro} through noncovalent binding (22), and has a high inhibition efficiency against SARS-CoV-2 (EC_{50} = 4.67 μM). These results suggest the potential of ebselen

Accepted preprint first posted on June 23, 2020. (Changes may still occur before final publication.)

for further study in COVID-19 treatment.

Given that SARS-CoV-2 mainly affects the lungs, studies have sought to explore drugs that are specifically suitable for inhalation. For example, the α-ketoamide 13b inhibitor has been optimized from α-ketoamide 11r, a previously designed drug with picomolar inhibitory activity against MERS-CoV in vitro (122), half-life enhancement in plasma, pronounced lung tropism, and is suitable for the inhalation route of administration (23). Zhang and colleagues solved the X-ray crystal structure of SARS-CoV-2 M^{pro} in complex with α-ketoamide 13b at 1.95 Å (PDB ID: 6Y2F) and 2.20 Å resolution (PDB ID: 6Y2G). The α-ketoamide 13b warhead interacts with the catalytic substrate-binding site of SARS-CoV-2 M^{pro} through two hydrogen bonding interactions, thus blocking the protease (IC_{50}, 900 nM; EC_{50}, 4–5 μM). Compared with other warheads, such as aldehydes (123) (compound 11a and 11b) and Michael acceptors (124) (compound N3), which only have one hydrogen bonding interaction with Cys145, α-ketoamide 13b has two hydrogen bonds, which help to lock the inhibitor in the catalytic site (122). α-ketoamide 13b in a nebulized form was tested in mice and found to be well-tolerated with no adverse effects (23), indicating that inhalational administration of this drug would be possible.

5.4. Targeting Viral Replication

The viral replication machinery, RNA-dependent RNA polymerase (RdRp), plays a pivotal role in genome replication. A number of small-molecule nucleoside analogues that mimic naturally occurring nucleosides have been designed to inhibit viral replication (**Figure 2*b,ii***). The RNA binding site on RdRp and the residues involved in the catalytic site are highly conserved among coronaviruses (125, 126). RdRp of SARS-CoV-2 shares 99.1% similarity and 96% amino acid sequence identity with SARS-CoV (127). These structural and functional features make RdRp a promising target for broad spectrum antivirals.

Remdesivir (GS-5734), a broad-spectrum antiviral drug originally developed against Ebola virus (128) by Gilead Sciences, Inc. Results from early clinical trials have shown that patients with advanced COVID-19 recover faster on remdesivir (129). In May 2020, the FDA approved remdesivir for emergency use in COVID-19 treatment (130). Remdesivir potently stops viral replication activity via RNA chain termination (128, 131). Using cryo-EM, Yin et al. solved the structure of remdesivir in complex with SARS-CoV-2 RdRp, a 50-base template-primer RNA at 2.5 Å resolution (PDB ID: 7BV2) (24). In this structure, the partial double-stranded RNA template is inserted into the central channel of RdRp, and remdesivir, covalently added into the

first replicated base pair, terminates chain elongation (**Figure 3*c***) (24).

RNA virus replication is also targeted by the cytidine analogue, β-D-N^4-hydroxycytidine (NHC), also known as EIDD-1931. NHC has been reported to have potent antiviral activities against RNA virus replication and the spread of Ebola, Hepatitis C, Marburg, Venezuelan equine encephalitis, influenza, murine hepatitis virus, and MERS-CoV (132–135), as well as against coronaviruses, including HCoV-NL63, SARS-CoV, and MERS-CoV (136–138). NHC inhibits SARS-CoV-2 replication in Vero cells (IC_{50} = 300 nM), Calu-3 cells (IC_{50} = 80 nM), and primary human airway epithelial cells (IC_{50} = 140 nM), with minimal cytotoxicity of CC_{50} > 10 μM (127). The inhibitory activity of coronavirus replication by NHC is consistent with an increased viral mutation rate (135, 139), an effect that is not observed with remdesivir. Sequence analysis on MERS-CoV-infected cells under NHC treatment revealed that the mutations that occur are mainly A:G and C:U transitions (127). In murine hepatitis virus, Phe480Leu and Val557Leu mutations in RdRp do not confer resistance to NHC, consistent with data showing that NHC exhibits only a low level of resistance with multiple viruses (133, 135, 139). Nucleoside analogues, such as ribavirin and 5-fluorouracil, are ineffective at targeting coronaviruses due to the proofreading function of the viral 3'-5' exoribonuclease (ExoN) that removes mismatched nucleosides (140, 141). NHC is only minimally affected by the ExoN proofreading function, suggesting that NHC overcomes the proofreading mechanism and inhibits the replication of coronaviruses.

Because NHC has broad antiviral activity against genetically distinct viruses, Toots et al. developed EIDD-2801, an isopropylester prodrug of NHC, which has improved oral bioavailability and pharmacokinetics in vivo (134). EIDD-2801 drives mutagenesis of viral RNA and causes increased codon change frequency, including stop codons. Thus, treatment with EIDD-2801 can reduce viral load in the lungs and improve pulmonary function in SARS-CoV- or MERS-CoV-infected mouse models (127). The high potency of NHC and EIDD-2801 against other coronaviruses and their oral bioavailability warrants the further study of these inhibitors to determine their safety, specificity, and efficacy against SARS-CoV-2 infection.

6. CONCLUSION

In this article, we have presented our analysis of the structural basis for SARS-CoV/CoV-2/MERS-receptor interactions and the potential for small-molecule inhibitors as therapeutics.

Comparing the independent and complex structures, the major therapeutic target is the NTD and RBD of S-protein of SARS-CoV-2, SARS-CoV, and MERS-CoV. Structural differences in the RBDs, the hACE2 binding loops, and the presence of the furin cleavage site may explain the higher transmissibility of SARS-CoV-2 and these differences could serve as important targets for drug design. Because of increased expression during infection, high sequence homology (90%) in comparison with SARS-CoV and lower mutation rate, SARS-CoV-2 nucleocapsid (N) proteins are emerging to be convenient vaccine targets (142, 143). Because the antibodies can only bind to cell-surface proteins, the relatively small size of the inhibitor compounds and their ability to target multiple viral pathways presents them as attractive molecules to treat COVID-19.

We highlight the relevance of small-molecule compounds that target two essential viral entry pathways: 1) the cathepsin B/L-dependent pathway, where inhibitors can be used to target cathepsin L, the endosomal proton pump, and autophagy; and 2) the protease-mediated plasma membrane entry pathway, where inhibitors can be designed to target TMPRSS2, furin, and the HR-driven, 6-HB complex formation. Additionally, M^{Pro} can be targeted to inhibit viral protein translation, and the inhibition of RNA replication machinery proteins, such as RdRp, can be designed to impede viral replication. Inhibitor compounds serve as templates for the design and optimization of new drugs, and the repurposing of already approved drugs with antiviral efficacy and specificity, thus allowing for a faster route to treatment options. The few drugs thus far in clinical trials have shown some efficacy, with the repurposed Ebola drug, remdesivir, paving the way as a lead drug for treating COVID-19 patients. Other drugs, such as the serine protease inhibitors camostat mesylate and nafamostat mesylate that target TMPRSS2, have exhibited efficacy that might lead to potential treatment options. Since most of the small-molecule inhibitors seem to target pathways other than blockade of binding of the virus to the hACE2 receptor, it is worth exploring a combination of recently identified SARS-CoV-2 neutralizing antibodies (47, 144) with inhibitor compounds as a combinatorial, multifaceted treatment approach against COVID-19. In vitro experimental data and clinical trial results presented thus far suggested that nafamostat mesylate and/or remdesivir are potential treatment options for COVID-19 patients. In addition to the use of these repurposed drugs for treatment, previous studies suggested the drugs' use as prophylactics. Nafamostat mesylate and remdesivir are shown to prevent endoscopic retrograde cholangiopancreatography (ERCP) (145) and MERS-CoV infection (146), respectively. Although these repurposed drugs show potential, it is unclear

which inhibitor might practically prevent and/or cure the disease.

Apart from the conventional viral protein directed strategies, alternative approaches to target the hACE2 receptor and other host cellular proteins may present promising outcomes as therapeutics and prophylactics against COVID-19. Decoy strategies involving the inhalation of modified soluble recombinant hACE2 and engineered inhibitors like hACE2 conjugated with fragment crystallizable (Fc) domains are being explored as COVID-19 treatment options (38, 147). As the alternative strategies may provide early protection by blocking SARS-CoV-2 S-glycoprotein/hACE2 WT interaction, it holds the potential to reduce the severe pathophysiological symptoms (acute lung injury, multi-organ failures) that result from cytokine storms and severe proinflammatory responses of COVID-19. Despite the advantages, these alternative options need extensive in vitro and in vivo testing before approval for treatment in patients.

Collectively, this review highlights a structural perspective on virus-receptor interactions and provides an up-to-date assessment of small-molecule compounds that inhibit coronaviruses, mainly SARS-CoV-2. The potential and newly identified compounds need to be extensively studied in animal models and placebo-controlled clinical trials to establish their efficacy and safety profiles against COVID-19. Given that this is a newly discovered virus, it is unclear what type of preventive or therapeutic strategy will be most relevant. As such, the quest for alternative prevention or treatment regimens against COVID-19 must continue progressively and dynamically.

DISCLOSURE STATEMENT

The authors are not aware of any affiliations, memberships, funding, or financial holdings that might be perceived as affecting the objectivity of this review.

ACKNOWLEDGMENTS

J.S. acknowledges partial support from Ministry of Education Singapore grants R154-000-A72-114 (Tier 1), R-154-000-B03-112 (Tier 2), and R-154-000-697-112 (Tier 3).

LITERATURE CITED

1. Li W, Hulswit RJG, Widjaja I, Raj VS, McBride R, et al. 2017. Identification of sialic acid-binding function for the Middle East respiratory syndrome coronavirus spike glycoprotein. *PNAS* 114(40):E8508–17
2. Wang, Zhang Y, Wu L, Niu S, Song C, et al. 2020. Structural and Functional Basis of SARS-CoV-2 Entry by Using Human ACE2. *Cell* 181(4):894–904.e9
3. Wrapp D, Wang N, Corbett KS, Goldsmith JA, Hsieh C, et al. 2020. Cryo-EM structure of the 2019-nCoV spike in the prefusion conformation. *Science* 367(6483):1260–63
4. Wu K, Li W, Peng G, Li F. 2009. Crystal structure of NL63 respiratory coronavirus receptor-binding domain complexed with its human receptor. *PNAS* 106(47):19970–74
5. Khan S, Siddique R, Shereen MA, Ali A, Liu J, et al. 2020. Emergence of a novel coronavirus, severe acute respiratory syndrome coronavirus 2: Biology and therapeutic options. *J. Clin. Microbiol.* 58(5):1–10
6. Zhou P, Yang X-L, Wang X-G, Hu B, Zhang L, et al. 2020. A pneumonia outbreak associated with a new coronavirus of probable bat origin. *Nature* 579(7798):270–73
7. Gorbalenya AE, Baker SC, Baric RS, de Groot RJ, Drosten C, et al. 2020. The species Severe acute respiratory syndrome-related coronavirus: classifying 2019-nCoV and naming it SARS-CoV-2. *Nat. Microbiol.* 5(4):536–44
8. Bojkova D, McGreig JE, McLaughlin K-M, Masterson SG, Widera M, et al. 2020. SARS-CoV-2 and SARS-CoV differ in their cell tropism and drug sensitivity profiles. *bioRxiv*
9. Brian D. Quinlan, Huihui Mou, Lizhou Zhang, Yan Guo WH, Ojha A, Mark, Parcells S, Luo G, et al. 2020. The SARS-CoV-2 receptor-binding domain elicits a potent neutralizing response without antibody-dependent enhancement. *Immunity* D-20–00389
10. Ou X, Liu Y, Lei X, Li P, Mi D, et al. 2020. Characterization of spike glycoprotein of SARS-CoV-2 on virus entry and its immune cross-reactivity with SARS-CoV. *Nat. Commun.* 11(1620):1–12
11. Li F. 2008. Structural analysis of major species barriers between humans and palm civets for severe acute respiratory syndrome coronavirus Infections. *J. Virol.* 82(14):6984–91
12. Walls AC, Park YJ, Tortorici MA, Wall A, McGuire AT, Veesler D. 2020. Structure, Function, and Antigenicity of the SARS-CoV-2 Spike Glycoprotein. *Cell* 181(2):281–292.e6
13. Coutard B, Valle C, de Lamballerie X, Canard B, Seidah NG, Decroly E. 2020. The spike glycoprotein of the new coronavirus 2019-nCoV contains a furin-like cleavage site absent in

CoV of the same clade. *Antivir. Res.* 176(104742):1–5

14. Srinivasan S, Cui H, Gao Z, Liu M, Lu S, et al. 2020. Structural genomics of SARS-COV-2 indicates evolutionary conserved functional regions of viral proteins. *Viruses* 12(4):360
15. Yuan Y, Cao D, Zhang Y, Ma J, Qi J, et al. 2017. Cryo-EM structures of MERS-CoV and SARS-CoV spike glycoproteins reveal the dynamic receptor binding domains. *Nat. Commun.* 8(15092):1–9
16. Wang N, Shi X, Jiang L, Zhang S, Wang D, et al. 2013. Structure of MERS-CoV spike receptor-binding domain complexed with human receptor DPP4. *Cell Res.* 23(8):986–93
17. Hofmann H, Pyrc K, Van Der Hoek L, Geier M, Berkhout B, Pöhlmann S. 2005. Human coronavirus NL63 employs the severe acute respiratory syndrome coronavirus receptor for cellular entry. *PNAS* 102(22):7988–93
18. Lan J, Ge J, Yu J, Shan S, Zhou H, et al. 2020. Structure of the SARS-CoV-2 spike receptor-binding domain bound to the ACE2 receptor. *Nature* 581(7807):215–20
19. Shang J, Ye G, Shi K, Wan Y, Luo C, et al. 2020. Structural basis of receptor recognition by SARS-CoV-2. *Nature* 581:221–24
20. Li F, Li W, Farzan M, Harrison SC. 2005. Structure of SARS coronavirus spike receptor-binding domain complexed with receptor. *J. Clin. Endocrinol. Metab.* 309:1864–68
21. Dai W, Zhang B, Su H, Li J, Zhao Y, et al. 2020. Structure-based design of antiviral drug candidates targeting the SARS-CoV-2 main protease. *Science* 368(6497):1331–35
22. Jin Z, Du X, Xu Y, Deng Y, Liu M, et al. 2020. Structure of Mpro from SARS-CoV-2 and discovery of its inhibitors. *Nature* 582(7811):289–93
23. Zhang L, Lin D, Sun X, Curth U, Drosten C, et al. 2020. Crystal structure of SARS-CoV-2 main protease provides a basis for design of improved α-ketoamide inhibitors. *Science* 368(6489):409–12
24. Wanchao Y, Chunyou M, Xiaodong L, Dan-Dan S, Qingya S, et al. 2020. Structural Basis for the Inhibition of the RNA-Dependent RNA Polymerase from SARS- CoV-2 by Remdesivir. *Science* eabc1560
25. Chou T. 2007. Stochastic entry of enveloped viruses: Fusion versus endocytosis. *Biophys. J.* 93(4):1116–23
26. Ou X, Liu Y, Lei X, Li P, Mi D, et al. 2020. Characterization of spike glycoprotein of SARS-CoV-2 on virus entry and its immune cross-reactivity with SARS-CoV. *Nat. Commun.*

11(1):1620

27. Wang H, Yang P, Liu K, Guo F, Zhang Y, et al. 2008. SARS coronavirus entry into host cells through a novel clathrin- and caveolae-independent endocytic pathway. *Cell Res.* 18(2):290–301
28. Matsuyama S, Nagata N, Shirato K, Kawase M, Takeda M, Taguchi F. 2010. Efficient Activation of the Severe Acute Respiratory Syndrome Coronavirus Spike Protein by the Transmembrane Protease TMPRSS2. *J. Virol.* 84(24):12658–64
29. Belouzard S, Chu VC, Whittaker GR. 2009. Activation of the SARS coronavirus spike protein via sequential proteolytic cleavage at two distinct sites. *PNAS* 106(14):5871–76
30. Qian Z, Dominguez SR, Holmes K V. 2013. Role of the Spike Glycoprotein of Human Middle East Respiratory Syndrome Coronavirus (MERS-CoV) in Virus Entry and Syncytia Formation. *PLOS ONE* 8(10):e76469
31. Gierer S, Bertram S, Kaup F, Wrensch F, Heurich A, et al. 2013. The Spike Protein of the emerging Betacoronavirus EMC uses a novel coronavirus receptor for entry, can be activated by TMPRSS2, and Is targeted by neutralizing antibodies. *J. Virol.* 87(10):5502–11
32. Glowacka I, Bertram S, Muller MA, Allen P, Soilleux E, et al. 2011. Evidence that TMPRSS2 Activates the Severe Acute Respiratory Syndrome Coronavirus Spike Protein for Membrane Fusion and Reduces Viral Control by the Humoral Immune Response. *J. Virol.* 85(9):4122–34
33. Iwata-Yoshikawa N, Okamura T, Shimizu Y, Hasegawa H, Takeda M, Nagata N. 2019. TMPRSS2 Contributes to Virus Spread and Immunopathology in the Airways of Murine Models after Coronavirus Infection. *J. Virol.* 93(6):1–15
34. Hoffmann M, Kleine-Weber H, Schroeder S, Krüger N, Herrler T, et al. 2020. SARS-CoV-2 Cell Entry Depends on ACE2 and TMPRSS2 and Is Blocked by a Clinically Proven Protease Inhibitor. *Cell* 181(2):271–280.e8
35. Hoffmann M, Kleine-Weber H, Pöhlmann S. 2020. A Multibasic Cleavage Site in the Spike Protein of SARS-CoV-2 Is Essential for Infection of Human Lung Cells. *Mol. Cell* 78(4):779–784.e5
36. Follis KE, York J, Nunberg JH. 2006. Furin cleavage of the SARS coronavirus spike glycoprotein enhances cell-cell fusion but does not affect virion entry. *Virology* 350(2):358–69

37. Yuki K, Fujiogi M, Koutsogiannaki S. 2020. COVID-19 pathophysiology: A review. *Clin. Immunol.* 215:108427
38. Jia HP, Look DC, Shi L, Hickey M, Pewe L, et al. 2005. ACE2 Receptor Expression and Severe Acute Respiratory Syndrome Coronavirus Infection Depend on Differentiation of Human Airway Epithelia. *J. Virol.* 79(23):14614–21
39. Towler P, Staker B, Prasad SG, Menon S, Tang J, et al. 2004. ACE2 X-Ray Structures Reveal a Large Hinge-bending Motion Important for Inhibitor Binding and Catalysis. *J. Biol. Chem.* 279(17):17996–7
40. Du L, Yang Y, Zhou Y, Lu L, Li F, Jiang S. 2017. MERS-CoV spike protien: a key target for antivirals. *Expert Opin. Ther. Targets* 21(2):131–43
41. Wan Y, Shang J, Graham R, Baric RS, Li F. 2020. Receptor Recognition by the Novel Coronavirus from Wuhan: an Analysis Based on Decade-Long Structural Studies of SARS Coronavirus. *J. Virol.* 94(7):1–9
42. Watanabe Y, Allen JD, Wrapp D, McLellan JS, Crispin M. 2020. Site-specific glycan analysis of the SARS-CoV-2 spike. *Science* eabb9983
43. Gui M, Song W, Zhou H, Xu J, Chen S, et al. 2017. Cryo-electron microscopy structures of the SARS-CoV spike glycoprotein reveal a prerequisite conformational state for receptor binding. *Cell Res*. 27(1):119–29
44. Kirchdoerfer RN, Wang N, Pallesen J, Wrapp D, Turner HL, et al. 2018. Stabilized coronavirus spikes are resistant to conformational changes induced by receptor recognition or proteolysis. *Sci. Rep.* 8(1):15701
45. Ju B, Zhang Q, Ge J, Wang R, Sun J, et al. 2020. Human neutralizing antibodies elicited by SARS-CoV-2 infection. *Nature*
46. Wrapp D, De Vlieger D, Corbett KS, Torres GM, Wang N, et al. 2020. Structural Basis for Potent Neutralization of Betacoronaviruses by Single-Domain Camelid Antibodies. *Cell* 181:1004–15
47. Wang C, Li W, Drabek D, Okba NMA, van Haperen R, et al. 2020. A human monoclonal antibody blocking SARS-CoV-2 infection. *Nat. Commun.* 11(1):2251
48. Harrison C. 2020. Coronavirus puts drug repurposing on the fast track. *Nat. Biotechnol.* 38(4):379–81
49. Guy RK, DiPaola RS, Romanelli F, Dutch RE. 2020. Rapid repurposing of drugs for

COVID-19. *Science* 368(6493):829–30

50. Jakubcová L, Hollỳ J, Varečková E. 2016. The role of fusion activity of influenza A viruses in their biological properties. *Acta Virol*. 60(2):121–35
51. Hamilton BS, Whittaker GR, Daniel S. 2012. Influenza virus-mediated membrane fusion: Determinants of hemagglutinin fusogenic activity and experimental approaches for assessing virus fusion. *Viruses* 4(7):1144–68
52. Mair CM, Ludwig K, Herrmann A, Sieben C. 2014. Receptor binding and pH stability - How influenza A virus hemagglutinin affects host-specific virus infection. *Biochim. Biophys. Acta - Biomembr.* 1838(4):1153–68
53. Shen LW, Mao HJ, Wu YL, Tanaka Y, Zhang W. 2017. TMPRSS2: A potential target for treatment of influenza virus and coronavirus infections. *Biochimie* 142:1–10
54. Simmons G, Gosalia DN, Rennekamp AJ, Reeves JD, Diamond SL, Bates P. 2005. Inhibitors of cathepsin L prevent severe acute respiratory syndrome coronavirus entry. *PNAS* 102(33):11876–81
55. Yang N, Shen HM. 2020. Targeting the Endocytic Pathway and Autophagy Process as a Novel Therapeutic Strategy in COVID-19. *Int. J. Biol. Sci.* 16(10):1724–31
56. Chen X, Wang K, Xing Y, Tu J, Yang X, et al. 2014. Coronavirus membrane-associated papain-like proteases induce autophagy through interacting with Beclin1 to negatively regulate antiviral innate immunity. *Protein Cell*. 5(12):912–27
57. Gassen NC, Niemeyer D, Muth D, Corman VM, Martinelli S, et al. 2019. SKP2 attenuates autophagy through Beclin1-ubiquitination and its inhibition reduces MERS-Coronavirus infection. *Nat. Commun.* 10(1):2–4
58. Gassen NC, Papies J, Bajaj T, Dethloff F, Emanuel J, et al. 2020. Analysis of SARS-CoV-2-controlled autophagy reveals spermidine, MK-2206, and niclosamide as putative antiviral therapeutics. *bioRxiv*. 2020.04.15
59. Dong X, Levine B. 2013. Autophagy and viruses: Adversaries or allies? *J. Innate Immun.* 5(5):480–93
60. Carmona-Gutierrez D, Bauer MA, Zimmermann A, Kainz K, Hofer SJ, et al. 2020. Digesting the crisis: autophagy and coronaviruses. *Microb. Cell* 7(5):119–28
61. Yao X, Ye F, Zhang M, Cui C, Huang B, et al. 2020. In Vitro Antiviral Activity and Projection of Optimized Dosing Design of Hydroxychloroquine for the Treatment of Severe

Acute Respiratory Syndrome Coronavirus 2 (SARS-CoV-2). *Clin. Infect. Dis.*, p. ciaa237

62. Wang M, Cao R, Zhang L, Yang X, Liu J, et al. 2020. Remdesivir and chloroquine effectively inhibit the recently emerged novel coronavirus (2019-nCoV) in vitro. *Cell Res*. 30:269–71
63. Liu J, Cao R, Xu M, Wang X, Zhang H, et al. 2020. Hydroxychloroquine, a less toxic derivative of chloroquine, is effective in inhibiting SARS-CoV-2 infection in vitro. *Cell Discov*. 6:16
64. Vincent MJ, Bergeron E, Benjannet S, Erickson BR, Rollin PE, et al. 2005. Chloroquine is a potent inhibitor of SARS coronavirus infection and spread. *Virol. J.* 2:69
65. Gao J, Tian Z, Yang X. 2020. Breakthrough: Chloroquine phosphate has shown apparent efficacy in treatment of COVID-19 associated pneumonia in clinical studies. *Biosci Trends* 14(1):72–73
66. Gautret P, Lagier J-C, Parola P, Hoang VT, Meddeb L, et al. 2020. Hydroxychloroquine and azithromycin as a treatment of COVID-19: results of an open-label non-randomized clinical trial. *Int. J. Antimicrob. Agents* 105949
67. Alhazzani W, Møller MH, Arabi YM, Loeb M, Gong MN, et al. 2020. Surviving Sepsis Campaign: guidelines on the management of critically ill adults with Coronavirus Disease 2019 (COVID-19). *Intensive Care Med*. 46(5):854–87
68. Dowall SD, Bewley K, Watson RJ, Vasan SS, Ghosh C, et al. 2016. Antiviral Screening of Multiple Compounds against Ebola Virus. *Viruses* 8(11):277
69. Elander B, Fellenius E, Leth R, Olbe L, Wallmark B. 1986. Inhibitory action of omeprazole on acid formation in gastric glands and on h+,k+-ATPase isolated from human gastric mucosa. *Scand. J. Gastroenterol.* 21(3):268–72
70. Long J, Wright E, Molesti E, Temperton N, Barclay W. 2015. Antiviral therapies against Ebola and other emerging viral diseases using existing medicines that block virus entry. *F1000Research* 4:30
71. Shin JM, Kim N. 2013. Pharmacokinetics and pharmacodynamics of the proton pump inhibitors. *J. Neurogastroenterol. Motil.* 19(1):25–35
72. Shang J, Wan Y, Luo C, Ye G, Geng Q, et al. 2020. Cell entry mechanisms of SARS-CoV-2. *PNAS* 117(21):11727–34
73. Huang IC, Bosch BJ, Li F, Li W, Kyoung HL, et al. 2006. SARS coronavirus, but not human

coronavirus NL63, utilizes cathepsin L to infect ACE2-expressing cells. *J. Biol. Chem.* 281(6):3198–203

74. Hoffmann M, Hofmann-Winkler H, Pöhlmann S. 2018. Priming time: How cellular proteases arm coronavirus spike proteins. *Act. Viruses by Host Proteases* 16:71–98
75. Eisenberg T, Knauer H, Schauer A, Büttner S, Ruckenstuhl C, et al. 2009. Induction of autophagy by spermidine promotes longevity. *Nat. Cell Biol.* 11(11):1305–14
76. Igarashi K, Kashiwagi K. 2010. Modulation of cellular function by polyamines. *Int. J. Biochem. Cell Biol.* 42(1):39–51
77. Morselli E, Mariño G, Bennetzen M V., Eisenberg T, Megalou E, et al. 2011. Spermidine and resveratrol induce autophagy by distinct pathways converging on the acetylproteome. *J. Cell Biol.* 192(4):615–29
78. Gupta VK, Scheunemann L, Eisenberg T, Mertel S, Bhukel A, et al. 2013. Restoring polyamines protects from age-induced memory impairment in an autophagy-dependent manner. *Nat. Neurosci.* 16(10):1453–60
79. Mounce BC, Olsen ME, Vignuzzi M, Connor JH. 2017. Polyamines and Their Role in Virus Infection. *Microbiol. Mol. Biol. Rev.* 81(4):e00029–17
80. Olsen ME, Filone CM, Rozelle D, Mire CE, Agans KN, et al. 2016. Polyamines and hypusination are required for ebolavirus gene expression and replication. *MBio* 7(4):e00882–16
81. Korovina AN, Tunitskaya VL, Khomutov MA, Simonian AR, Khomutov AR, et al. 2012. Biogenic polyamines spermine and spermidine activate rna polymerase and inhibit RNA helicase of hepatitis c virus. *Biochemistry* 77(10):1172–80
82. Mounce BC, Poirier EZ, Passoni G, Simon-Loriere E, Cesaro T, et al. 2016. Interferon-Induced Spermidine-Spermine Acetyltransferase and Polyamine Depletion Restrict Zika and Chikungunya Viruses. *Cell Host Microbe.* 20(2):167–77
83. Wang RC, Wei Y, An Z, Zou Z, Xiao G, et al. 2012. Akt-mediated regulation of autophagy and tumorigenesis through Beclin 1 phosphorylation. *Science* 338(6109):956–59
84. Degtyarev M, De Mazière A, Orr C, Lin J, Lee BB, et al. 2008. Akt inhibition promotes autophagy and sensitizes PTEN-null tumors to lysosomotropic agents. *J. Cell Biol.* 183(1):101–16
85. Jurgeit A, McDowell R, Moese S, Meldrum E, Schwendener R, Greber UF. 2012.

Niclosamide Is a Proton Carrier and Targets Acidic Endosomes with Broad Antiviral Effects. *PLOS Pathog*. 8(10):e10002976

86. Jeon S, Ko M, Lee J, Choi I, Byun SY, et al. 2020. Identification of antiviral drug candidates against SARS-CoV-2 from FDA-approved drugs. *Antimicrob. Agents Chemother.* AAC.00819-:
87. Ditzel J, Schwartz M. 1967. Worm Cure Without Tears: The effect of niclosamide on taeniasis saginata in man. *Acta Med. Scand.* 182(5):663–64
88. World Health Organization, Stuart MC, Kouimtzi M, Hill SR. 2009. WHO model formulary 2008 / editors: Marc C. Stuart, Maria Kouimtzi, Suzanne R. Hill. World Health Organization
89. Bestle D, Heindl MR, Limburg H, van TVL, Pilgram O, et al. 2020. TMPRSS2 and furin are both essential for proteolytic activation and spread of SARS-CoV-2 in human airway epithelial cells and provide promising drug targets. *bioRxiv*. 2020.04.15.042085
90. Lu L, Liu Q, Zhu Y, Chan KH, Qin L, et al. 2014. Structure-based discovery of Middle East respiratory syndrome coronavirus fusion inhibitor. *Nat. Commun.* 5:3067
91. Liu S, Xiao G, Chen Y, He Y, Niu J, et al. 2004. Interaction between heptad repeat 1 and 2 regions in spike protein of SARS-associated coronavirus: Implications for virus fusogenic mechanism and identification of fusion inhibitors. *Lancet* 363(9413):938–47
92. Bosch BJ, Martina BEE, Van Der Zee R, Lepault J, Haijema BJ, et al. 2004. Severe acute respiratory syndrome coronavirus (SARS-CoV) infection inhibition using spike protein heptad repeat-derived peptides. *PNAS* 101(22):8455–60
93. Gibo J, Ito T, Kawabe K, Hisano T, Inoue M, et al. 2005. Camostat mesilate attenuates pancreatic fibrosis via inhibition of monocytes and pancreatic stellate cells activity. *Lab. Investig* 85(1):75–89
94. Marotta F, Fesce E, Rezakovic I, De Chui H, Suzuki K, Idéo G. 1994. Nafamostat mesilate on the course of acute pancreatitis. *Int. J. Pancreatol.* 16(1):51–59
95. Hoffmann M, Schroeder S, Kleine-Weber H, Müller MA, Drosten C, Pöhlmann S. 2020. Nafamostat mesylate blocks activation of SARS-CoV-2: New treatment option for COVID-19. *Antimicrob. Agents Chemother.* 64(6):e00754–20
96. Yamamoto M, Matsuyama S, Li X, Takeda M, Kawaguchi Y, et al. 2016. Identification of Nafamostat as a Potent Inhibitor of Middle East Respiratory Syndrome Coronavirus S Protein-Mediated Membrane Fusion Using the Split-Protein-Based Cell-Cell Fusion Assay.

Antimicrob. Agents Chemother. 60(11):6532–39

97. Zhirnov OP, Matrosovich TY, Matrosovich MN, Klenk HD. 2011. Aprotinin, a protease inhibitor, suppresses proteolytic activation of pandemic H1N1v influenza virus. *Antivir. Chem. Chemother.* 21(4):169–74
98. Meyer D, Sielaff F, Hammami M, Böttcher-Friebertshäuser E, Garten W, Steinmetzer T. 2013. Identification of the first synthetic inhibitors of the type II transmembrane serine protease TMPRSS2 suitable for inhibition of influenza virus activation. *Biochem. J.* 452(2):331–43
99. Xia S, Yan L, Xu W, Agrawal AS, Algaissi A, et al. 2019. A pan-coronavirus fusion inhibitor targeting the HR1 domain of human coronavirus spike. *Sci. Adv.* 5(4):eaav4580
100. Xia S, Liu M, Wang C, Xu W, Lan Q, et al. 2020. Inhibition of SARS-CoV-2 (previously 2019-nCoV) infection by a highly potent pan-coronavirus fusion inhibitor targeting its spike protein that harbors a high capacity to mediate membrane fusion. *Cell Res.* 30(4):343–55
101. Xia S, Zhu Y, Liu M, Lan Q, Xu W, et al. 2020. Fusion mechanism of 2019-nCoV and fusion inhibitors targeting HR1 domain in spike protein. *Cell. Mol. Immunol.* 11:1–3
102. Zhu Y, Yu D, Yan H, Chong H, He Y. 2020. Design of potent membrane fusion inhibitors against SARS-CoV-2, an emerging coronavirus with high fusogenic activity. *J. Virol.* JVI.00635–20
103. Zhu Y, Chong H, Yu D, Guo Y, Zhou Y, He Y. 2019. Design and Characterization of Cholesterylated Peptide HIV-1/2 Fusion Inhibitors with Extremely Potent and Long-Lasting Antiviral Activity. *J. Virol.* 93(11):e02312–18
104. Chong H, Zhu Y, Yu D, He Y. 2018. Structural and Functional Characterization of Membrane Fusion Inhibitors with Extremely Potent Activity against Human Immunodeficiency Virus Type 1 (HIV-1), HIV-2, and Simian Immunodeficiency Virus. *J. Virol.* 92(20):e01088–18
105. Anand K, Ziebuhr J, Wadhwani P, Mesters JR, Hilgenfeld R. 2003. Coronavirus main proteinase (3CLpro) Structure: Basis for design of anti-SARS drugs. *Science* 300(5626):1763–67
106. Hegyi A, Ziebuhr J. 2002. Conservation of substrate specificities among coronavirus main proteases. *J. Gen. Virol.* 83(Pt 3):595–99
107. Xue X, Yu H, Yang H, Xue F, Wu Z, et al. 2008. Structures of Two Coronavirus Main

Proteases: Implications for Substrate Binding and Antiviral Drug Design. *J. Virol.* 82(5):2515–27

108. Ren Z, Yan L, Zhang N, Guo Y, Yang C, et al. 2013. The newly emerged SARS-Like coronavirus HCoV-EMC also has an "Achilles'' heel": Current effective inhibitor targeting a 3C-like protease." *Protein Cell* 4(4):248–50
109. Wang F, Chen C, Tan W, Yang K, Yang H. 2016. Structure of Main Protease from Human Coronavirus NL63: Insights for Wide Spectrum Anti-Coronavirus Drug Design. *Sci. Rep.* 22677
110. Lee CC, Kuo CJ, Ko TP, Hsu MF, Tsui YC, et al. 2009. Structural basis of inhibition specificities of 3C and 3C-like proteases by zinc-coordinating and peptidomimetic compounds. *J. Biol. Chem.* 284(12):7646–55
111. Hilgenfeld R. 2014. From SARS to MERS: crystallographic studies on coronaviral proteases enable antiviral drug design. *FEBS J.* 281(18):4085–96
112. Fehr AR, Perlman S. 2015. Coronaviruses: An overview of their replication and pathogenesis. *Coronaviruses Methods Protoc.* 1282:1–23
113. Yang H, Xie W, Xue X, Yang K, Ma J, et al. 2005. Design of wide-spectrum inhibitors targeting coronavirus main proteases. *PLOS Biol.* 3(10):e324
114. Anand K, Palm GJ, Mesters JR, Siddell SG, Ziebuhr J, Hilgenfeld R. 2002. Structure of coronavirus main proteinase reveals combination of a chymotrypsin fold with an extra α-helical domain. *EMBO J.* 21(13):3213–24
115. Kil J, Lobarinas E, Spankovich C, Griffiths SK, Antonelli PJ, et al. 2017. Safety and efficacy of ebselen for the prevention of noise-induced hearing loss: a randomised, double-blind, placebo-controlled, phase 2 trial. *Lancet* 390(10098):969–79
116. Masaki C, Sharpley AL, Cooper CM, Godlewska BR, Singh N, et al. 2016. Effects of the potential lithium-mimetic, ebselen, on impulsivity and emotional processing. *Psychopharmacology (Berl.)* 233(14):2655–61
117. Singh N, Halliday AC, Thomas JM, Kuznetsova O, Baldwin R, et al. 2013. A safe lithium mimetic for bipolar disorder. *Nat. Commun.* 4:1332
118. Sakamoto J, Oba K, Matsui T, Kobayashi M. 2006. Efficacy of oral anticancer agents for colorectal cancer. *Dis. Colon Rectum.* 49(10 SUPPL.):S82–91
119. Morimoto K, Koh M. 2003. Postoperative adjuvant use of carmofur for early breast cancer.

Osaka City Med. J. 49(2):77–83

120. Nishio S, Kishimoto T, Maekawa M, Kawakita J, Morikawa Y, et al. 1987. Study on effectiveness of carmofur (Mifurol®) for urogenital carcinoma, especially bladder cancer, as a post-operative adjuvant chemotherapeutic agent. *Hinyokika Kiyo* 33(2):295–303
121. Gröhn P, Heinonen E, Kumpulainen E, Lansimies H, Lantto A, et al. 1990. Oral carmofur in advanced gastrointestinal cancer. *Am. J. Clin. Oncol. Cancer Clin. Trials* 13(6):477–79
122. Zhang L, Lin D, Kusov Y, Nian Y, Ma Q, et al. 2020. α-Ketoamides as Broad-Spectrum Inhibitors of Coronavirus and Enterovirus Replication: Structure-Based Design, Synthesis, and Activity Assessment. *J. Med. Chem.* 63(9):4562–78
123. Zhu L, George S, Schmidt MF, Al-Gharabli SI, Rademann J, Hilgenfeld R. 2011. Peptide aldehyde inhibitors challenge the substrate specificity of the SARS-coronavirus main protease. *Antiviral Res*. 92(2):204–12
124. Tan J, George S, Kusov Y, Perbandt M, Anemuller S, et al. 2013. 3C Protease of Enterovirus 68: Structure-Based Design of Michael Acceptor Inhibitors and Their Broad-Spectrum Antiviral Effects against Picornaviruses. *J. Virol.* 87(8):4339–51
125. Te Velthuis AJW. 2014. Common and unique features of viral RNA-dependent polymerases. *Cell. Mol. Life Sci.* 71(22):4403–20
126. Venkataraman S, Prasad BVLS, Selvarajan R. 2018. RNA dependent RNA polymerases: Insights from structure, function and evolution. *Viruses* 10(2):76
127. Sheahan TP, Sims AC, Zhou S, Graham RL, Pruijssers AJ, et al. 2020. An orally bioavailable broad-spectrum antiviral inhibits SARS-CoV-2 in human airway epithelial cell cultures and multiple coronaviruses in mice. *Sci. Transl. Med.* 12(541):eabb5883
128. Tchesnokov EP, Feng JY, Porter DP, Götte M. 2019. Mechanism of inhibition of ebola virus RNA-dependent RNA polymerase by remdesivir. *Viruses* 11(4):326
129. National Institutes of Health. 2020. *NIH clinical trial shows Remdesivir accelerates recovery from advanced COVID-19* [Press release]. Retrieved from https://www.nih.gov/news-events/news-releases/nih-clinical-trial-shows-remdesivir-accelerates-recovery-advanced-covid-19
130. Food and Drug Administration (FDA). 2020. Coronavirus (COVID-19) Update: FDA Issues Emergency Use Authorization for Potential COVID-19 Treatment. [Press Announc.]. Retrieved from https://www.fda.gov/news-events/press-announcements/coronavirus-covid-

19-update-fda-issues-emergency-use-authorization-potential-covid-19-treatment

131. Gordon CJ, Tchesnokov EP, Woolner E, Perry JK, Feng JY, et al. 2020. Remdesivir is a direct-acting antiviral that inhibits RNA-dependent RNA polymerase from severe acute respiratory syndrome coronavirus 2 with high potency. *J. Biol. Chem.* 295(20):6785–679

132. Reynard O, Nguyen XN, Alazard-Dany N, Barateau V, Cimarelli A, Volchkov VE. 2015. Identification of a new ribonucleoside inhibitor of ebola virus replication. *Viruses* 8(5):137

133. Stuyver LJ, Whitaker T, McBrayer TR, Hernandez-Santiago BI, Lostia S, et al. 2003. Ribonucleoside analogue that blocks replication of bovine viral diarrhea and hepatitis C viruses in culture. *Antimicrob. Agents Chemother.* 47(1):244–54

134. Toots M, Yoon JJ, Cox RM, Hart M, Sticher ZM, et al. 2019. Characterization of orally efficacious influenza drug with high resistance barrier in ferrets and human airway epithelia. *Sci. Transl. Med.* 11(515):1–14

135. Urakova N, Kuznetsova V, Crossman DK, Sokratian A, Guthrie DB, et al. 2017. β-D- N 4 -Hydroxycytidine Is a Potent Anti-alphavirus Compound That Induces a High Level of Mutations in the Viral Genome. *J. Virol.* 92(3):e01965–17

136. Pyrc K, Bosch BJ, Berkhout B, Jebbink MF, Dijkman R, et al. 2006. Inhibition of human coronavirus NL63 infection at early stages of the replication cycle. *Antimicrob. Agents Chemother.* 50(6):2000–2008

137. Barnard DL, Hubbard VD, Burton J, Smee DF, Morrey JD, et al. 2004. Inhibition of severe acute respiratory syndrome-associated coronavirus (SARSCoV) by calpain inhibitors and β-D-N4-hydroxycytidine. *Antivir. Chem. Chemother.* 15(1):15–22

138. Agostini ML, Pruijssers AJ, Chappell JD, Gribble J, Lu X, et al. 2019. Small-Molecule Antiviral β-D- N 4 -Hydroxycytidine Inhibits a Proofreading-Intact Coronavirus with a High Genetic Barrier to Resistance. *J. Virol.* 93(24):e01348–19

139. Yoon JJ, Toots M, Lee S, Lee ME, Ludeke B, et al. 2018. Orally efficacious broad-spectrum ribonucleoside analog inhibitor of influenza and respiratory syncytial viruses. *Antimicrob. Agents Chemother.* 62(8):e00766–18

140. Smith EC, Blanc H, Vignuzzi M, Denison MR. 2014. Coronaviruses Lacking Exoribonuclease Activity Are Susceptible to Lethal Mutagenesis: Evidence for Proofreading and Potential Therapeutics. *PLOS Pathog.* 10(7):e1004342

141. Ferron F, Subissi L, De Morais ATS, Le NTT, Sevajol M, et al. 2017. Structural and

molecular basis of mismatch correction and ribavirin excision from coronavirus RNA. *PNAS* 115(2):E162–71

142. Padron-Regalado E. 2020. Vaccines for SARS-CoV-2: Lessons from Other Coronavirus Strains. *Infect. Dis. Ther.* 9(2):255–74

143. Dutta NK, Mazumdar K, Gordy JT. 2020. The Nucleocapsid Protein of SARS-CoV-2: a Target for Vaccine Development. *J. Virol.* 94(13):e00647–20

144. Jiang S, Hillyer C, Du L. 2020. Neutralizing Antibodies against SARS-CoV-2 and Other Human Coronaviruses. *Trends Immunol*. 41(5):355–59

145. Jae HC, In SL, Hyung KK, Yu KC, Jae MP, et al. 2009. Nafamostat for prophylaxis against post-endoscopic retrograde cholangiopancreatography pancreatitis compared with gabexate. *Gut Liver*. 3(3):205–10

146. de Wit E, Feldmann F, Cronin J, Jordan R, Okumura A, et al. 2020. Prophylactic and therapeutic remdesivir (GS-5734) treatment in the rhesus macaque model of MERS-CoV infection. *PNAS* 117(12):6771–76

147. Ameratunga R, Lehnert K, Leung E, Comoletti D, Snell R, et al. 2020. Inhaled modified angiotensin converting enzyme 2 (ACE2) as a decoy to mitigate SARS-CoV-2 infection. *N. Z. Med. J.* 133(1515):112–18

148. Hoffmann M, Kleine-Weber H, Schroeder S, Krüger N, Herrler T, et al. 2020. SARS-CoV-2 Cell Entry Depends on ACE2 and TMPRSS2 and Is Blocked by a Clinically Proven Protease Inhibitor. *Cell* 181(2):271–280.e8

149. Wu CJ, Jan JT, Chen CM, Hsieh HP, Hwang DR, et al. 2004. Inhibition of severe acute respiratory syndrome coronavirus replication by niclosamide. *Antimicrob. Agents Chemother.* 48(7):2693–96

150. Kawase M, Shirato K, van der Hoek L, Taguchi F, Matsuyama S. 2012. Simultaneous Treatment of Human Bronchial Epithelial Cells with Serine and Cysteine Protease Inhibitors Prevents Severe Acute Respiratory Syndrome Coronavirus Entry. *J. Virol.* 86(12):6537–45

151. Kassell B, Radicevic M, Ansfield MJ, Laskowski M. 1965. The basic trypsin inhibitor of bovine pancreas IV. The linear sequence of the 58 amino acids. *Biochem. Biophys. Res. Commun.* 18:255–58

152. Jin Z, Zhao Y, Sun Y, Zhang B, Wang H, et al. 2020. Structural basis for the inhibition of SARS-CoV-2 main protease by antineoplastic drug Carmofur. *Nat. Struct. Mol. Biol.*

27(6):529–32

153. Sheahan TP, Sims AC, Graham RL, Menachery VD, Gralinski LE, et al. 2017. Broad-spectrum antiviral GS-5734 inhibits both epidemic and zoonotic coronaviruses. *Sci. Transl. Med.* 9(396):eaal3653

154. European Medicines Agency. 2020. *Summary on compassionate use Remdesivir Gilead*. European Medicines Agency [Press release]. Retrieved from https://www.ema.europa.eu/en/news/ema-recommends-expanding-remdesivir-compassionate-use-patients-not-mechanical-ventilation

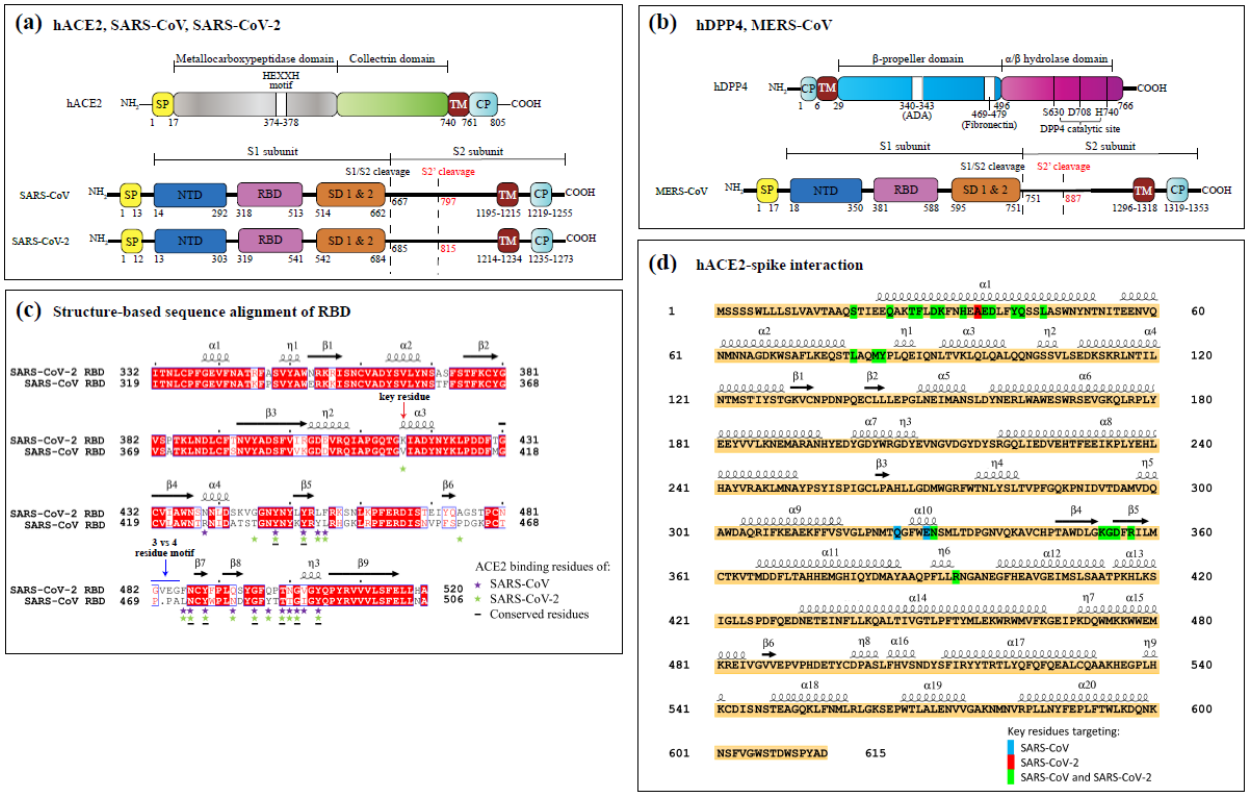

Figure 1 Sequence comparison of host cell receptor (hACE2/hDPP4), SARS-CoV, and SARS-CoV-2. (a) Domain architecture of the SARS-CoV and SARS-CoV-2 spike glycoprotein and host cell receptor hACE2. (b) Domain architecture of the MERS-CoV spike glycoprotein and host cell receptor hDPP4. SP (signal peptide); TM (transmembrane); CP (cytoplasmic tail); NTD (N-terminal domain); RBD (receptor binding domain); SD (subdomain); FP (fusion peptide). (c) Structure-based sequence alignment of SARS-CoV RBD and SARS-CoV-2 RBD. The secondary structure (α for helix; η for 310 helix; and β for strand) are assigned based on PDB code 6LZG. Conserved residues are highlighted in red and similar residues lettered in red. SARS-CoV and SARS-CoV-2 residues interacting with hACE2 are marked with purple star and green star, respectively. The conserved residues are underlined in black. The key residue Lys417 in SARS-CoV-2 and its equivalent, valine in SARS-CoV are indicated using a red arrow. The 3-residue motif in SARS-CoV and 4-residue motif in SARS-CoV-2 are indicated using a blue arrow. Sequence alignment was performed using ClustalW and the figure was prepared using ESPript (Robert and Gouet, 2014). (d) hACE2 (1–615aa) was assigned using STRIDE (Heinig and Frishman, 2004) with PDB code 1R42, and the secondary structures are shown in the sequence. The key residues interacting with SARS-CoV and SARS-CoV-2 are highlighted in blue and red, respectively. The binding residues conserved in SARS-CoV and SARS-CoV-2 are highlighted in green.

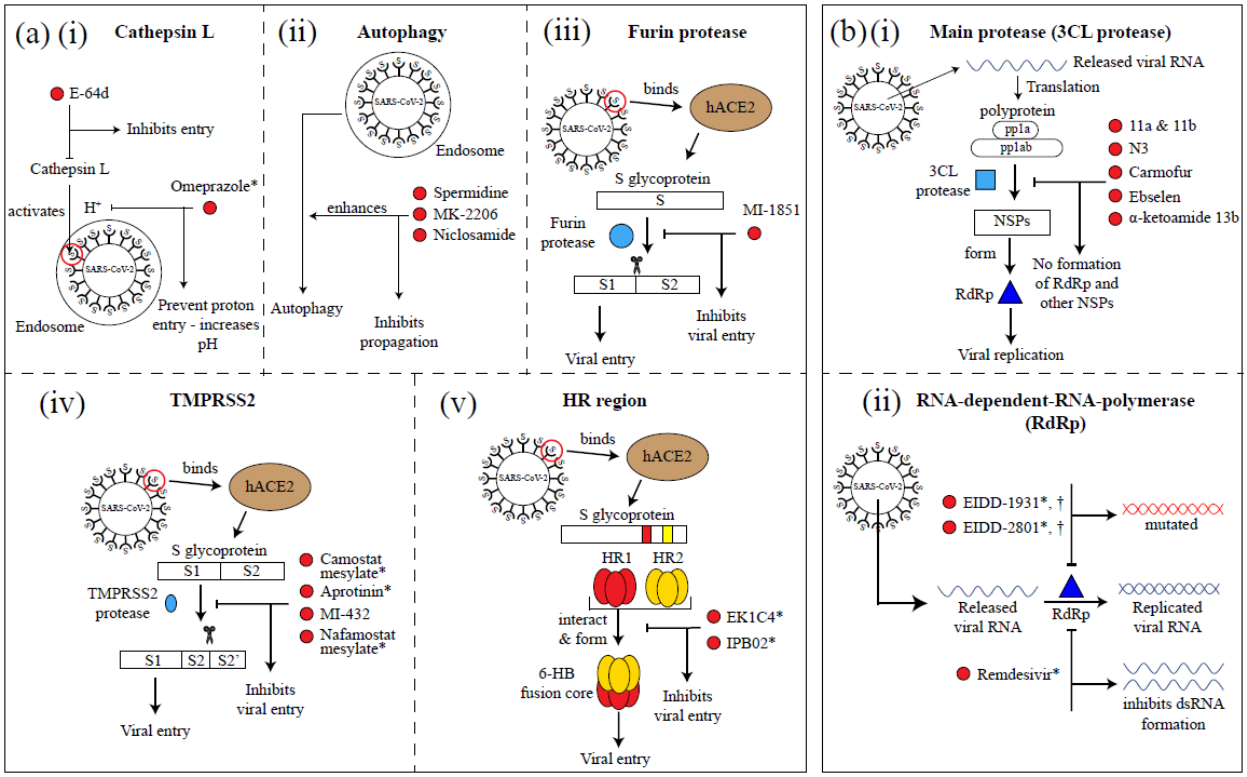

Figure 2 Blocking of host-pathogen interaction by small molecule inhibitors. (a) Inhibitors targeting (i) Cathepsin L, (ii) autophagy pathway, (iii) Furin protease, (iv) TMPRSS2 protease, and (v) formation of 6-HB fusion core during virus entry and fusion. (b) Inhibitors targeting (i) main proteases, and (ii) RdRp during virus replication. Inhibitors targeting SARS-CoV-2 and SARS-CoV are marked using asterisk (*), and those targeting SARS-CoV-2 and MERS-CoV are marked using dagger (†).

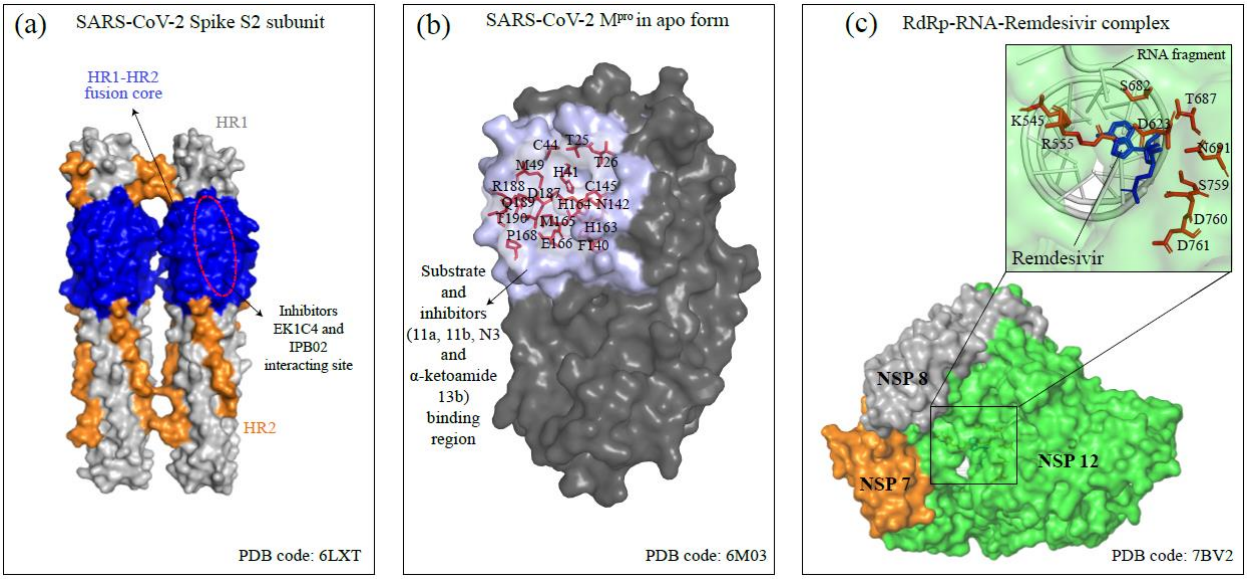

Figure 3 Interaction of inhibitors. (a) Molecular surface representation of Heptad-region (HR) in spike S2 subunit showing HR1 (gray) and HR2 (orange). HR1-HR2 fusion core is showing in blue. Inhibitors EK1C4 and IPB02, binding to HR1 fusion core is highlighted using red-dotted oval. Inhibitors interactng with HR1 fusion core prevents formation of 6HB core. (b) Molecular surface representation of SARS-CoV-2 protease (3CL protease) with substrate and inhibitor binding region highlighted using red sticks. Inhibitors, 11a, 11b, N3 and α-ketoamide 13b, target the substrate binding region that inhibits the formation of NSPs, marked in light blue. (c) Molecular surface representation of RdRp complex interacting with RNA fragment and inhibitors Remdesivir. NSP 12, NSP 7 and NSP 8 are highlighted in green, orange and gray, respectively. NSP 12, 7 and 8 interact to form RdRp. RNA fragment and Remdesivir are shown in cartoon and blue sticks, respectively. The key binding residues of RdRp interacting with Remdesivir are shown in red sticks, and residues are labeled in black.

Table 1 Host receptor and CoV S-protein interactions

Host Protein (receptor)	Pathogen Protein (CoV S)	Binding Affinity (Method)				Host - Pathogen Interaction Region	Other Remarks	Structure (Resolution) - References
		Host receptor construct	Pathogen CoV-S construct	Affinity (KD - nM)	Method			
hACE2	SARS-CoV-2 S	NTD (19–615)	RBD (319–541)	4.7	SPR	Residues of hACE2 NTD interacts with SARS-CoV-2 RBD and S1 subdomain	'RRAR' furin cleavage site at the S1/S2 subunit. Gln493, Leu455 of CoV-2 S RBD stabilize Lys31 in hACE2. SARS-CoV-2 RBDs have a higher affinity for hACE2 than SARS-CoV RBD Abs target S2 subunit in the S protein	PDB 6M0J (X-ray 2.45 Å) (18) PDB 6VW1 (X-ray 2.68 Å) (19) PDB 6LZG (X-ray 2.5 Å) (2) PDB 6VYB (S protein ectodomain, open state, cryo-EM 3.2 Å) (12) PDB 6VXX (S protein, closed state, cryo-EM 2.8 Å) EMDB 21457 (S protein ectodomain, open state, cryoEM 3.2 Å) EMDB 21452 (S protein, closed state, cryo-EM 2.8 Å)
		NTD (1–615)	Trimer (1–1208)	14.7	SPR			
		NTD (1–615)	RBD-SD1 (319–591)	34.6	SPR			
		NTD (19–615)	S1 (1–685)	94.6 ± 6.5	SPR			
		NTD (1–615)	RBD (319–529)	44.2	SPR			
		NTD (1–614)	S1 (1–685)	1.2 ± 0.1	BLI			
TMPRSS2 ; hACE2	SARS-CoV-2 S	N.A				hACE2 interacts with RBD	Serine protease TMPRSS2 is used as a	(12, 148)

						of SARS-CoV-2	cofactor by SARS-CoV-2 Asn501 in CoV S RBD stabilize Lys353 in hACE2.	
human/civet hACE2	SARS-CoV S	NTD (16–615)	RBD (306–575)	31	SPR	Residues in the hACE2 NTD interacts with SARS-CoV RBD and S1 subdomain	SARS-CoV S RBD mutations (Asn479Lys, Thr487Ser) reduces binding affinity to ACE2 by multiple folds. Strong salt-bridge between Arg426 (S RBD) and Glu329 (hACE2)	PDB 3D0G (X-ray 2.8 Å) (11) PDB 2AJF (X-ray 2.9 Å) (20)
		NTD (1–615)	RBD (306–515)	185	SPR			
		NTD (19–615)	RBD (306–527)	408.7 ± 11	SPR			
		NTD (1–614)	S1 (1–676)	15	BLI			
hDPP4 (or CD26)	MERS-CoV S	hDPP4 (39–766)	RBD (367–606)	12	SPR	Residues in the β-propeller domain at the N-term of DPP4 interacts with MERS-CoV RBD domain	Mutation Tyr499Ala in MERS-CoV S disrupts binding to DPP4	PDB 4L72 (X-ray 3 Å) (16)
		hDPP4 (39–766)	RBD (36–606)	6.4 ± 0.8	SPR			

Abbreviations: CoV S, Spike (S) protein situated on the surface of SARS-CoV, SARS-CoV-2, and MERS virus that interact with host receptors; RBD, Receptor binding domain; hACE2, human angiotensin-converting enzyme 2; human/civet, N-terminal helix from civet and the peptidase domain from human; SPR, Surface plasmon resonance; NTD, N-terminal domain; CTD, C-terminal domain; K_D, Dissociation constant; BLI, Biolayer Interferometry; DPP4, dipeptidyl peptidase 4; MERS, Middle East Respiratory Syndrome; SARS, Severe Acute Respiratory Syndrome; SARS-CoV-2 S trimer, Residues 1–1208 with residues 986 and 987 substituted with prolines, a 'GSAS' substitution at the furin cleavage site residues 682–685, a fused C-terminal T4 fibritin trimerization motif.

Table 2 Inhibitors targeting the viral entry and fusion

Serial no.; Name (references); MW (g/mol); Target region	**Chemical Structure**	**Activity IC_{50} and Function**	**Status of therapeutics developments (in progress)**	**Other details- IC_{50}; CC_{50}**
1. **Omeprazole** (8) **MW: 345.40** **Lysosome**	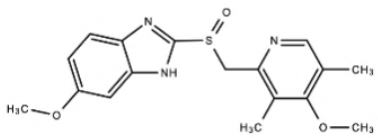	SARS-CoV-2: 34 µM SARS-CoV: 26.8 µM -As a proton pump inhibitor, increases pH in the lysosome. -Inhibits double-stranded RNA formation.	Repurposed drug SARS-CoV-2: In vitro Experiments	CC_{50} > 80 µM
2. **E-64d** (26, 72, 73) **MW: 342.43** **Lysosomal cathepsin and calpain**	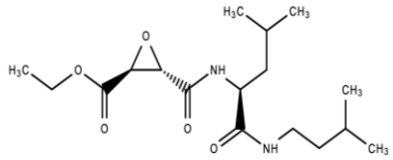	N.A -Inhibits lysosomal cathepsin B/L and blocks the cathepsin/endosome entry pathway of SARS-CoV-2.	Repurposed drug SARS-CoV-2: In combination with camostat mesylate. In vitro Experiments	N.A
3. **Spermidine** (58) **MW: 145.25** **Autophagy pathway**	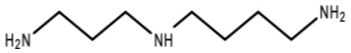	SARS-CoV-2: 149 µM -Acts as an autophagy inducer, enhances autophagy and inhibits SARS-CoV-2 propagation.	Repurposed drug SARS-CoV-2: In vitro Experiments	N.A

4. **MK-2206** (58) **MW: 407.50** **Autophagy pathway**	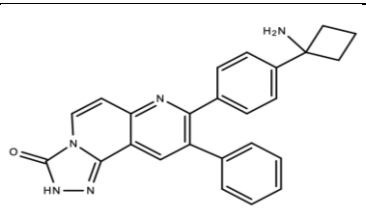	SARS-CoV-2: 90 nM -Inhibits AKT1, enhances autophagy and inhibits SARS-CoV-2 propagation.	Repurposed drug SARS-CoV-2: In vitro Experiments	N.A
5. **Niclosamide** (58, 86, 149) **MW: 327.12** **Autophagy pathway**	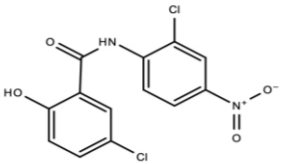	SARS-CoV-2: 170–280 nM -Inhibits E3-ligase S-phase kinase-associated protein 2 (SKP2), enhances autophagy and inhibits SARS-CoV-2 propagation.	Repurposed drug SARS-CoV-2: In vitro Experiments	N.A
6. **MI-1851** (89) **MW: 767.90** **Furin protease**	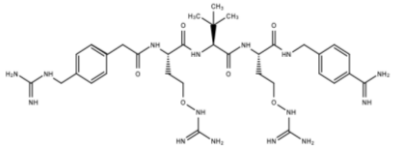	N.A -Prevents virus entry by inhibiting furin cleavage at S1/S2 site of S protein.	Repurposed drug SARS-CoV-2: In vitro Experiments	N.A
7. **Camostat mesylate** (8, 34, 95, 150) **MW: 494.50** **TMPRSS2 protease**	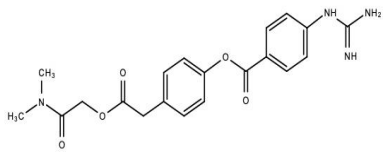 CH_3SO_3H	SARS-CoV-2: 1.2 µM SARS-CoV: 16.7 µM -Partially blocks SARS-CoV-2-S- and SARS-CoV-driven entry by inhibiting the protease TMPRSS2. -Fully blocks the SARS-2-S-driven entry when applied together with inhibitor E-64d.	Repurposed drug SARS-CoV-2: In clinical trial	SARS-CoV-2: EC_{50} = 87 nM SARS-CoV: EC_{50} = 198 nM CC_{50} > 200 µM

8. **Nafamostat mesylate** (73, 95, 96) **MW: 539.60** **TMPRSS2 protease**	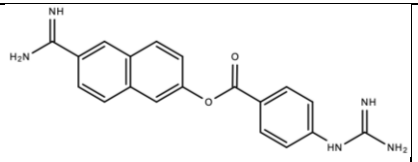 2 CH_3SO_3H	SARS-CoV-2: 0.49 μM SARS-CoV: 18.9 μM -Prevents the S protein activation by inhibiting TMPRSS2 protease.	Repurposed drug SARS-CoV-2: In clinical trial	**SARS-CoV-2**: EC_{50} = 5 nM; **SARS-CoV**: EC_{50} = 1.4 nM CC_{50} >200 μM
9. **Aprotinin** (8, 89, 151) **MW: 6511.51** **TMPRSS2 protease**	N'- RPDFCLEPPYTGPCKARII RY FYNAKAGLCQTFVYGGC RA KRNNFKSAEDCMRTCGG A-C'	SARS-CoV-2: 22.9 KIU/ml SARS-CoV:118 KIU/ml -Prevents virus entry by inhibiting the TMPRSS2 cleavage at the S2 site of S protein. -Inhibits double-stranded RNA formation in SARS-CoV-2 infected cells.	Repurposed drug SARS-CoV-2: In vitro Experiments	CC_{50} > 1,000 KIU
10. **MI-432** (89, 98) **MW: 573.57** **TMPRSS2 protease**	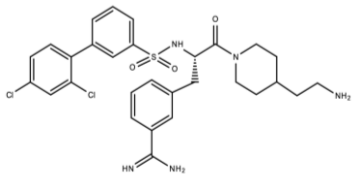	N/A -Prevents virus entry by inhibiting TMPRSS2 cleavage at S2 site of S protein.	Repurposed drug SARS-CoV-2: In vitro Experiments	N.A
11. **EK1C4** (100) **MW: 5258.06** **Spike protein**	N'- EK1 - GSGSG – PEG4 – Chol -C' Where EK1 is N'- SLDQINVTFLDLEYEMKK LE	SARS-CoV-2 S protein-mediated membrane fusion: 1.3 nM SARS-CoV-2 pseudovirus: 15.8 nM Live SARS-CoV-2:	New drug SARS-CoV-2: In vitro and in vivo Experiments	CC_{50} >5 μM SI > 136

	EAIKKLEESYIDLKEL -C’	36.5 nM - Inhibits cell-cell fusion by binding to HR1 region in the S2 subunit of S protein and prevent the six-helical bundle fusion core structure formation.		
12. **IPB02** (102) **MW: 4408.23** **Spike protein**	N’- ISGINASVVNIQKEIDRLN EV AKNLNESLIDLQELK(Chol) -C’	SARS-CoV-2 S protein-mediated membrane fusion: 25 nM SARS-CoV-2 pseudovirus: 80 nM SARS-CoV-pseudovirus: 251 nM - Inhibits cell-cell fusion by binding to HR1 region in the S2 subunit of S protein and prevent the six-helical bundle fusion core structure formation.	New drug SARS-CoV-2: In vitro Experiments	N.A

Abbreviations: MW, Molecular weight; Chol, cholesterol; HR1, heptad repeat 1; KIU, Kallikrein Inactivator Units; EC_{50}, half maximal effective concentration; CC_{50}, half maximal cytotoxic concentration; SI, selective index.

MW for no. 6, 10 are calculated based on the chemical structure; no. 9, 11, 12 are computed from Expasy (http://web.expasy.org); no. 1, 2, 3, 4, 5, 7, 8 are obtained from PubChem (https://pubchem.ncbi.nlm.nih.gov).

Table 3 Inhibitors targeting the Main viral protease and RdRp

Serial no.; Name (references); MW (g/mol); Target region	**Chemical Structure**	**Activity IC_{50} and Function**	**Status of therapeutics developments (in progress)**	**Other details - complex PDB code (resolution); EC_{50}; CC_{50}**
1. Lead compound 11a, 11b (21) MW of 11a: 452.56; 11b: 464.50 Main protease	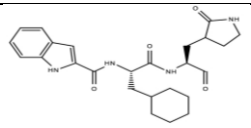 11a 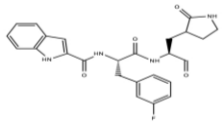 11b	SARS-CoV-2: 40–53 nM -Occupies the substrate-binding pocket and covalently binds to Cys145, blocks the enzyme activity of M^{pro}.	New drug SARS-CoV-2: In vitro and in vivo Experiments	6LZE (1.5 Å) 6M0K (1.5 Å) EC_{50} = 0.53–0.72 μM CC_{50} >100 μM
2. N3 (22, 107, 108) MW: 680.35 Main protease	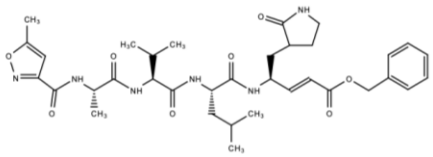	N.A -Binds to the substrate-binding pocket and irreversibly inhibits M^{pro} activity.	Repurposed drug SARS-CoV-2: In vitro Experiments	6LU7 (2.16 Å) 7BQY (1.7 Å) EC50 = 16.77 μM

3. Carmofur (22, 152) MW: 257.26 Main protease	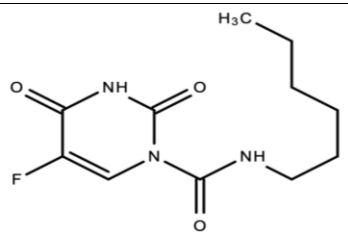	SARS-CoV-2: 1.82 μM -Covalently binds to C145 of the catalytic dyad M^{pro}, completely modifies M^{pro}.	Repurposed drug SARS-CoV-2: In vitro Experiments	7BUY (1.60 Å) EC_{50} = 24.30 μM CC_{50} = 133.4 μM SI = 5.36
4. Ebselen (22) MW: 274.20 Main protease	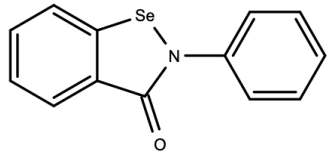	SARS-CoV-2: 670 nM -Covalently or noncovalently binds to C145 of the catalytic dyad M^{pro}, partially modifies M^{pro}.	Repurposed drug SARS-CoV-2: In vitro Experiments	EC_{50} = 4.67 μM
5. α-ketoamide 13b (23) MW: 580.66 Main protease	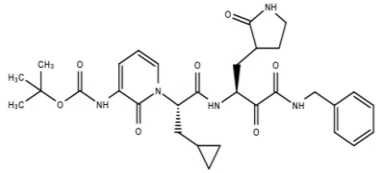	SARS-CoV-2: 670 nM -Binds to substrate-binding pocket.	New drug SARS-CoV-2: In vitro and in vivo Experiments	6Y2F (1.95 Å) 6Y2G (2.20 Å) EC_{50} = 4–5 μM
6. Remdesivir (GS-5734) (8, 24, 146, 153, 154) MW: 602.60 RdRp	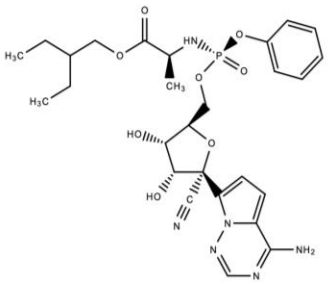	SARS-CoV-2: 0.31 μM SARS-CoV: 0.11 μM -As an adenosine analogue, remdesivir binds to RdRp and incorporates into nascent viral RNA chains and results	Repurposed drug SARS-CoV-2: In clinical trial -It inhibits replication of SARS-CoV and MERS-CoV in tissue culture and nonhuman animal model.	7BV2 (2.5 Å)

		in premature termination. -Inhibit formation of double-stranded RNA		
7. β-D-*N*^{4}-hydroxycytidine (NHC) or EIDD-1931 (127, 135) MW: 259.22 EIDD-2801 (prodrug of NHC) (127, 134) MW: 329.31 RdRp	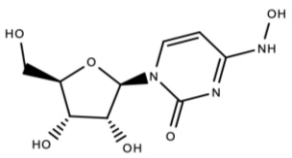 NHC 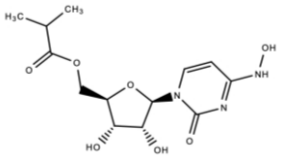 EIDD-2801	SARS-CoV-2: 80–300 nM MERS-CoV: 150 nM -As a ribonucleoside analog, NHC potently inhibits MERS-CoV and SARS-CoV-2 replication by increasing the mutation rate in viral genomic RNA.	Repurposed drug SARS-CoV-2: In vitro and in vivo Experiments -It has a broad-spectrum antiviral activity against SARS-CoV-2, MERS-CoV, SARS-CoV, and related zoonotic group 2b or 2c Bat-CoVs.	CC_{50} >10 μM EIDD-2801: Improved oral bioavailability in non- human primates.

Abbreviations: MW, Molecular weight; EC_{50}, half maximal effective concentration; CC_{50}, half maximal cytotoxic concentration; SI, selective index; RdRp, RNA-dependent RNA polymerase.

MW for no. 1, 5 are calculated based on the chemical structure; no. 2, 3, 4, 6, 7 are obtained from PubChem (https://pubchem.ncbi.nlm.nih.gov).

TERMS AND DEFINITIONS

hACE2: human Angiotensin-converting enzyme 2

hDPP4: Human Dipeptidyl peptidase 4

TMPRSS2: Transmembrane protease serine 2

RdRp: RNA-dependent RNA polymerase

NTD: N-terminal domain

CTD: C-terminal domain

RBD: Receptor binding domain

RBM: Receptor binding motif

PDB ID(s): Protein Data Bank unique identifier

SPR: Surface plasmon resonance

BLI: Bio-layer Interferometry

SKP2: S-phase kinase-associated protein 2

SARS-CoV-2: Severe acute respiratory syndrome-related coronavirus-2

SARS-CoV: Severe acute respiratory syndrome-related coronavirus

MERS-CoV: Middle East respiratory syndrome-related coronavirus

S: Spike

TPC2: Two-pore channel subtype 2

PIKfyve: Phosphatidylinositol 3-phosphate 5-kinase

HR: Heptad repeat

ExoN: Exoribonuclease

ERCP: Endoscopic retrograde cholangiopancreatography

Fc: Fragment crystallizable

N: Nucleocapsid